INNER AND OUTER FLOW VELOCITY DISTRIBUTIONS THROUGH TALL SIMULATED VEGETATION (U)

Technical Report

by

S. Ito

FLUID MECHANICS PROGRAM
ENGINEERING RESEARCH CENTER
COLLEGE OF ENGINEERING
COLORADO STATE UNIVERSITY
FORT COLLINS, COLORADO

CER67-68JEC61

INNER AND OUTER FLOW VELOCITY DISTRIBUTIONS THROUGH TALL SIMULATED VEGETATION (U)

Technical Report

by

S. Ito

U. S. Army Research Grant
DA-AMC-28-043-65-G20

Fluid Dynamics and Diffusion Laboratory
Engineering Research Center
College of Engineering
Colorado State University
Fort Collins, Colorado

Distribution of this Report
is unlimited

The findings in this report are not to be construed
as an official Department of the Army position.

April 1968 CER67-68JEC61

ABSTRACT

The velocity distribution in and above model vegetation is the subject of this study. Experiments have revealed that flow over a surface which has been made rough by covering it with tall simulated plants may have a universal distribution law. It is suggested that this law can be expressed in terms of the two parameters $\left(\frac{\Delta u}{V_*}\right)_{max}$ and η_o, which in turn depend on the shape, height, and spacing of the covering elements.

TABLE OF CONTENTS

LIST OF TABLES

LIST OF FIGURES

LIST OF FIGURES - Continued

DEFINITION OF TERMS

Notation	Definition
A, B, C, D	Constants occurring in logarithmic laws for turbulent layers
b	Batchelor constant
C_f	Skin-friction coefficient
C_s	Skin-friction function
f	Stream functions for turbulent profiles
$h = \frac{2}{20}$	Shear distribution function
k	Karman constant
K_r	Size of particle composing the least rough surface
$R_x = \frac{u_a x}{\nu}$	Dimensionless downwind distance
$R_\delta = \frac{u_a \delta}{\nu}$	Dimensionless boundary-layer thickness
u_a	Velocity of ambient air stream
u	Velocity in x-direction
V_*	Friction velocity
w	Velocity in Z-direction
X, x	Downwind distance from origin of turbulent boundary-layer
X'	Distance downwind from edge of simulated vegetation area
Z	Height above surface

DEFINITION OF TERMS (Continued)

Notation	Definition
Z_o	Roughness length
$\frac{\Delta u}{V_*}$	Shift in logarithmic profile caused by roughness
δ	Boundary thickness
η	Dimensionless height (Z/δ)
η_o	Edge of wake
ν	Kinematic viscosity

Chapter I

INTRODUCTION

The first analytical description of the velocity distribution within a vegetative canopy was formulated by Tan and Ling (Lemon 1963). Cionco et al. (1963) also made an attempt to describe this profile with an analytical formula. Inoue (1963) proposed that the canopy eddy has a scale that is independent of the height above the ground. He also suggested that the coefficient of momentum absorption is independent of the plant height. These two assumptions lead to exponential velocity profiles within canopies.

Experimental investigations of turbulent structures in and above canopies may be carried out in two ways: (a) taking field data at numerous measuring points, or (b) constructing a simulated canopy and subjecting it to laboratory tests. In many cases, the costs associated with method "a" are excessively large. This cost factor motivated personnel of the Fluid Dynamics and Diffusion Laboratory to adopt method "b". Results of these investigations using the Army meteorological wind tunnel (Fig. 1-1) were presented by Plate and Quraishi (1965) and Cermak and Plate (1963). These results showed that the flow may be divided into two types: (a) inner flow and (b) outer flow at a certain height. For instances, it was found that the tall elements modified the flow in the layer above the effective plant

height. This phenomenon can be seen in Figs. 4-3 through 4-5. Thus, the disturbance associated with the flow over a plant extends into the whole boundary layer.

The purpose of this study is to develop significant parameters that will express the universal profile which appears over an area covered with vegetation. Wind tunnel results indicate that vertical profiles depend upon the location of the measuring device with respect to the individual roughness elements. However, in order to simplify the analysis, we shall consider the mean motion to be two-dimensional.

Chapter II

EXPERIMENTAL EQUIPMENT AND PROCEDURE

Experiments employed two types of roughness elements: (a) flexible plastic strips, and (b) wooden dowels. The plastic strips were 0.25 in. wide, 0.0075 in. thick and 4 in. high. These roughness elements were attached to wooden strips with their broad sides facing the direction of the wind. Spacing in the direction normal to the flow was one element per linear inch, and spacing in the direction of flow was one row every 2 inches. The arrangement of the flexible strips is shown in Fig. 2-1. Dowels, each being 2 in. high and 3/16 in. in diameter, were arranged in a square pattern 1 in. on a side, as shown in Fig. 2-2.

All experimental data were obtained at the Fluid Dynamics and Diffusion Laboratory located at Colorado State University. A detailed description of all experimental equipment can be found in the paper by Plate and Quraishi (1965).

Chapter III

TURBULENT BOUNDARY LAYER

The purpose of this study is to investigate the boundary-layer velocity profiles for flow over a rough surface consisting of tall elements. In order to prepare a suitable foundation for such a discussion, we shall first re-examine the conventional formulations for smooth and rough walls.

Velocity data in turbulent boundary layers over smooth walls are normally expressed in one of three ways:

$$\frac{u}{u_a} = \left(\frac{Z}{\delta}\right)^n \tag{3.1}$$

$$\frac{u - u_a}{V_*} = A \log \frac{Z}{\delta} + B \tag{3.2}$$

$$\frac{u}{V_*} = A \log \frac{ZV_*}{\nu} + C \quad . \tag{3.3}$$

We are then faced with the problem of determining the friction velocity and boundary-layer thickness from mean velocity data obtained in the laboratory.

Equation (3.1) may be evaluated from measurements of velocity in the boundary layer as a function of the distance from the surface. Plotted velocity profiles, using $\frac{u}{u_a}$ versus Z/δ, do not coincide, but form a family of profiles for different Reynolds numbers. For an example refer to the experimental data plotted by Clauser (1954) as

seen in Fig. 3-1. Thus, in place of the single universal profile that exists for laminar layers, turbulent layers make families of profiles depending on both Reynolds numbers and the degree of roughness of the wall. Although, there is a wide-spread belief that profiles in a turbulent boundary layer are well represented by a single 1/7-power curve, experimental data indicate that the exponent varies from one-third to one-tenth, belying the existence of a single curve. The above results have been substantiated for geophysical flows by studies probing the atmospheric boundary layer for a neutral condition.

Equation (3.2), often referred to as the "universal velocity defect," relates wall effects and free stream effects. This relationship introduces both the wall shear stress and the boundary-layer thickness. However, data plotted on this basis correlates in the outer part of the boundary layer, but not near the wall. Equation (3.3) must be applied for flow descriptions near the wall.

It is difficult to determine the flow's undisturbed boundary-layer thickness, δ, and the wall shear stress, V_*, from laboratory data. However, it is the intent of this paper to describe turbulent processes over a vegetated area in terms of these parameters. Universal constants, including those appearing in Equations (3.2) and (3.3) can be found with a reasonable amount of accuracy. The unknown variables, δ and V_*, can then be determined by combining these two equations.

The universal profile-function for the turbulent layer is assumed to be of the form

$$\frac{u - u_a}{V_*} = - f'(\eta)$$

where $\eta = \frac{Z}{\delta}$

and $$V_* = \left(\frac{\tau_o}{\rho} \right)^{1/2} , \qquad (3.4)$$

where f is essentially a stream function and its derivative f' represents the universal velocity profile. If Equation (3.4) is substituted into the continuity equation for two-dimensional, incompressible flow, one obtains the following equation for the vertical velocity:

$$w = V_* \frac{d\delta}{dx} (f - \eta f') , \qquad (3.5)$$

where $f(0) = 0$. (In this report, it will be assumed that V_* is independent of position over a region of the canopy sufficiently far from the ends where the flow has become established.)

Equations (3.4) and (3.5), are then substituted into the boundary-layer equation for zero pressure gradient,

$$u \frac{\partial u}{\partial x} + w \frac{\partial u}{\partial Z} = \frac{1}{\rho} \frac{\partial \tau}{\partial Z} . \qquad (3.6)$$

This operation is identical to Clauser's presentation, which is expressed by

$$\frac{d\delta}{dx}\left(\frac{u_a}{V_*}\,\eta f'' - f f''\right) = \frac{\partial}{\partial\eta}\,h\,, \tag{3.7}$$

where $h = \frac{\tau}{\tau_o}$.

Equation (3.7) is then integrated across the turbulent boundary layer.

$$\frac{d\delta}{dx}\int_0^1 \left(\frac{u_a}{V_*}\,\eta f'' - f f''\right) d\eta = h_{\eta=1} - 1\,. \tag{3.8}$$

Since $h_{\eta=1} = 0$, a relation between the turbulent boundary-layer thickness , δ , and the wall shear stress, V_* , is given by

$$\frac{d\delta}{dx} = \frac{1}{\left\{\frac{u_a}{V_*}\,f(1) - \int_0^1 f'^2(\xi)\,d\xi\right\}}\,. \tag{3.9}$$

The wall shear stress is determined from Equations (3.2) and (3.3), which overlap within the turbulent boundary layer. In the overlap zone, for a smooth plate, a relation between these factors may be obtained by the elimination u and Z by subtraction, yielding

$$\frac{u_a}{V_*} = A \log \frac{\delta V_*}{\nu} + C - B\,. \tag{3.10}$$

Equation (3.10) can be rewritten as

$$\frac{u_a}{V_*} = A \log \frac{\delta u_a}{\nu}\,\frac{V_*}{u_a} + C - B\,; \tag{3.11}$$

or

$$C_s + A \log C_s = A \log R_\delta + C - B \quad , \tag{3.12}$$

where $C_s = \frac{u_a}{V_*}$, $R_\delta = \frac{\delta u_a}{\nu}$, $A = 5.75$, $C = 5.5$, and $B = -2.5$.

The above mentioned values for the universal constants should be acceptable in the presentation which follows.

C_s can be expressed in terms of a local friction coefficient, C_f , by the following relation:

$$C_s = \sqrt{\frac{2}{C_f}} \quad . \tag{3.13}$$

To integrate Equation (3.8), Equation (3.12) must be rearranged to obtain a simple relation between C_s and R_δ . Although Equation (3.12) does not contain an explicit relation for C_s in terms of R_δ , an approximation procedure can be used to obtain such a relation (see Appendix). Equation (3.12) is replaced by

$$C_s = \beta \quad A \log (R_\delta + 2.5) - A \log (2.5 + D) + D \quad , \tag{3.14}$$

where $\beta = \frac{1}{1.08}$, and $D = C - B$. This equation contains a coefficient adjusted for Equation (3.12). The differences between Equations (3.12) and (3.14) are verified by a numerical calculation shown in Fig. 3-2. The result is acceptable as an approximation.

After substituting Equation (3.14) into Equation (3.9), and then integrating the results, we obtain a relation between the downwind distance and the boundary-layer thickness for a smooth surface:

$$R_x = R_\delta \left[43.92 \log (R_\delta + 2.5) - 123.85 \right] + 109.80 \log (R_\delta + 2.5) - 41.10. \quad (3.15)$$

To examine Equation (3.15), wind tunnel data were plotted in the dimensionless form seen in Fig. 3-3; additional data of Poreh and Cermak (1963) are shown in Fig. 3-4.

Although Equations (3.14) and (3.15) are in agreement with the small amount of experimental data that is available, these equations need to be compared with other studies of boundary-layer flow. Karman (1921) applied a modified form of the logarithmic law to the calculation of the skin-friction drag of a flat plate. He accomplished this by means of the momentum equation (see for an example, Goldstein (ed.), Modern Developments in Fluid Dynamics, p. 362). For large values of $k \frac{u_a}{V_*}$ the approximation is:

$$C_f^{-1/2} = A' + B' \log (R_x C_f) \quad . \quad (3.16)$$

The theoretically predicted relation was found to be in good agreement with the experiment performed by Kampf (1929). Equations (3.14) and (3.15) were used to determine the range of R_x for which $C_f^{-1/2}$ varies linearly with $\log (R_x C_f)$. Fig. 3-5 shows that the linear relation is valid for large values of R_x .

Since nearly all boundary surfaces with which the atmosphere comes in contact are aerodynamically rough, it is desirable to investigate the general problem of flow over a rough surface. The equation for an inner profile of a small rough surface can be written as:

$$\frac{u}{V_*} = A \log \frac{V_* Z}{\nu} + C - \frac{\Delta u}{V_*} , \qquad (3.17)$$

where $\frac{\Delta u}{V_*}$ represents the vertical shift of the logarithmic curve caused by a small amount of roughness. Usually this shift is considered to be a function of the Reynolds number $R_{k_r} = \frac{K_r u_a}{\nu}$ However, for any given roughness, the equation does not show a unique value, and as such is regarded as an experimental constant with a certain ambiguity. This ambiguity forces the investigator to determine the position roughness by two other factors: (a) the dimensions such as height, width, and spacing of the roughness elements, and (b) the statistical configuration. When R_{k_r} is large and the viscous flow region is highly disturbed, the inner layer is usually considered independent of the viscosity. $\frac{\Delta u}{V_*}$ is often expressed as

$$\frac{\Delta u}{V_*} = A \log \frac{V_* k_r}{\nu} + D . \qquad (3.18)$$

The above mentioned method for rough surfaces of small elements may be applied to surfaces with tall elements. In other words, $\frac{\Delta u}{V_*}$ caused by tall elements is expected to be associated with

the same phenomena as an area covered with vegetation. Figure 3-6 illustrates the change in wind speed downwind of an area with tall elements. Experimental data may also be applied to the discernible roughness length Z_o as will be illustrated later in this study. At the present time, it is sufficient to state that the original flow will be modified by two factors: (a) the downwind distance, and (b) the amount of flow penetration into the area with the tall elements.

The formula for a field with a small amount of roughness is:

$$\frac{u}{V_*} = A \log \frac{Z}{Z_o} \quad , \tag{3.19}$$

where $Z_o = \gamma k_r$ and γ is a certain constant which is dependent upon the specific shape of the roughness elements. However, Equation (3.19) is the formula accepted by most investigators even though it reflects some of the above mentioned ambiguity.

The outer and inner parts of the turbulent boundary layer are represented as follows:

$$\frac{u - u_a}{V_*} = A \log \frac{Z}{\delta} + B \tag{3.20}$$

$$\frac{u}{V_*} = A \log \frac{Z}{Z_o} \quad . \tag{3.21}$$

Equations (3.20) and (3.21) indicate an overlap zone that is defined as:

$$\frac{u_a}{V_*} = A \log \frac{\delta}{Z_o} - B \quad . \tag{3.22}$$

Equation (3.22) contains a skin-friction law for a small rough plate that differs from the relation of a smooth plate, Equation (3.11). Changing the notation, Equation (3.22) can be written as:

$$C_s = A \log \frac{\delta}{Z_o} - B \quad . \tag{3.23}$$

After substituting Equation (3.23) into Equation (3.9), we obtain the result

$$\frac{x}{Z_o} = \frac{\delta}{Z_o} \left(47.44 \log \frac{\delta}{Z_o} - 61.81\right) \quad . \tag{3.24}$$

Equation (3.24) expresses a relationship between the downwind distance and the boundary-layer thickness. This relationship is shown in Fig. 3-7. It should be noticed that Equation (3.24) is similar to an expression of "plume-width," which grows with an increase of the neutral layer's downwind distance (see Cermak 1963, Batchelor 1964). Downwind variations in the turbulent boundary-layer thickness are attributable to momentum losses at the boundary.

Equation (3.24) may be expressed in the following familiar form:

$$b\,k \frac{x}{Z_o} = \frac{\delta}{Z_o} \left(\log \frac{\delta}{Z_o} - E\right) \quad , \tag{3.25}$$

where $b\,k = \frac{1}{47.44}$ and $E = 1.3$. Both of these factors are obtained from Equation (3.24). Equation (3.25) corresponds to a characteristic plume-width seen in the turbulent diffusion of particles released

at a chimney height of zero elevation. It is feasible to assign a value to the Batchelor constant b . This is accomplished by referring to the 0.4 portion of the Karman constant. The Batchelor constant "b" should be nearly equal to k as shown in the relation $b\,k \simeq \frac{1}{47.44}$. The only external parameter that appears in the above formulation then is constant for the wind profile in a turbulent boundary layer. It should be mentioned that the foregoing discussion is based on the situation in which the momentum transfer differs from the mass transfer.

The foregoing results are supported by a linear relationship between $C_f^{-1/2}$ and $\log \left(C_f^{1/2} \cdot \frac{x}{Z_o} \right)$. This relationship was found by Karman (1934), and is expressed by:

$$C_f^{-1/2} = A'' + B'' \log \left(C_f^{1/2} \cdot \frac{x}{Z_o} \right) \qquad (3.26)$$

Equations (3.23) and (3.24) have been used to construct Fig. 3-8. Equation (3.26) is in good agreement with the curve for

$$\log \left(C_f^{1/2} \frac{x}{Z_o} \right) > 4.0 \quad .$$

Chapter IV

EXPERIMENTAL DATA AND ANALYSIS

Prior to discussing the experimental data, a few of the characteristics of the wind tunnel should be noted. Calibration data using an ambient velocity of $u_a = 30$ ft/sec is plotted in Fig. 4-1. On this plot, "x" represents the distance downwind from the leading edge. Figure 4-1 also indicates that the upper and lower layers have different slopes. It is believed that this difference in slopes was the result of a stimulator generating a leading edge within the wind tunnel. Also, investigators found that the upper layer dominated the overall tunnel flow. This fact made it difficult to obtain a reasonable boundary thickness from the theory discussed in Chapter III. To fulfill the requirements of the theory, the flow's roughness height Z_o was determined by using the slope of the upper layer, as shown in Table 1.

Once Z_o has been found, both the thickness of the boundary-layer and the friction velocity can be obtained for a given distance downwind by Equations (3.23) and (3.24). Wind-tunnel parameters are also shown in Table 1. In this discussion, the boundary-layer thickness, "δ", corresponds to the distance from the tunnel floor to that level where the local velocity reaches a value of approximately

$0.92\,u_a$. It should be noted that u_a is the velocity outside of the boundary layer. The value assigned to this factor is not what is normally expected, but the difference has no substantial effect on the outcome of test results. One area where this difference may be important is in regard to a constant, such as the "B" constant, which is included in a logarithmic profile. In this particular example, the velocity, $u - u_a$, does not become zero at $Z/\delta = 1$.

TABLE 1

VALUES OF PARAMENTERS FOR THE FLOW OVER A PLATE WITH A ROUGH SURFACE OF SMALL ELEMENTS

u_a = 30 ft/sec				$Z_o = 2.2 \times 10^{-2}$ in.			
x ft	10	20	30	40	50	60	70
δ in.	3.07	4.29	5.97	7.59	9.00	10.38	12.10
V_* ft/sec	2.32	2.23	2.11	2.01	1.97	1.91	1.89

The profile, using reference parameters shown in Table 1, may be expressed universally, as illustrated in Fig. 4-2. It should be remembered that this profile reflects the domination of the upper boundary layer, and that this deviation from the norm is regarded as a characteristic of the wind tunnel.

Data were taken from tests in which tall simulated plants were placed at the leading edge of a given flow. This flow was mixed by two influences: (a) the growing turbulent boundary layer above a rough surface of small elements, and (b) the turbulence that was caused by the tall elements. These two factors may appear inseparable, but for the purposes of this discussion they are considered individually.

Experiments were conducted using two types of rough surfaces of tall elements as discussed in the introduction. Raw data, from the flexible plastic strips and the peg elements, are plotted with different ambient velocities in Figs. 4-3, 4-4, and 4-5. In these figures, "x" denotes the distance from the leading edge of the small elements, and "x" denotes the distance from the leading edge of the tall elements. Disturbance in the flow extended throughout the boundary-layer.

The flow's roughness height "Z_o" is determined by finding how much the slope of the upper layer deviates from the profile in front of the rough area of tall elements. This value is then substituted into Equations (3.29) and (3.23) which yield the values of δ and V_* seen in Tables 2, 3, and 4.

Note that the character of the roughness height "Z_o" for the same surface depends upon the ambient velocity values tabulated in Tables 1, 2, 3, and 4. This fact is reflected in Fig. 4-6. Resulting from this fact is the hypothesis that "Z_o" can be used to develop a reference scale that will yield a similarity law between model and

prototype (see Cermak, 1963). Tani (1963) found this same phenomenon in his investigations of the atmospheric boundary layer.

TABLE 2

VALUES OF δ AND V_*

CALCULATED FROM THE EXPERIMENTAL DATA

FOR FLEXIBLE PLASTIC STRIPS

	u_a = 10 ft/sec				Z_o = 1.15×10^{-2} in.				
x ft	36	40	42	46	50	52	54	56	58
x' ft	-4	0	2	6	10	12	14	16	18
δ in.	12.5	13.3	13.5	14.1	14.9	15.1	15.8	16.0	16.3
V_* ft/sec	0.830	0.826	0.821	0.810	0.801	0.797	0.790	0.781	0.781

TABLE 3

VALUES OF δ AND V_*

CALCULATED FROM THE EXPERIMENTAL DATA

FOR FLEXIBLE PLASTIC STRIPS

	u_a = 20 ft/sec				Z_o = 1.80×10^{-2} in.				
x ft	36	40	42	46	50	52	54	56	58
x' ft	-4	0	2	6	10	12	14	16	18
δ in.	6.64	7.23	7.60	8.10	8.30	8.62	9.40	9.50	10.10
V_* ft/sec	1.34	1.31	1.31	1.28	1.28	1.27	1.26	1.26	1.25

All available experimental data were plotted Figs. 4-7, 4-8, and 4-9. Plotting was accomplished by applying the universal defect law which employs the parameters in Tables 2, 3, and 4. These figures indicate that the profile is still in the transition range at the edge of the simulated vegetation area. Thus, the discussion of the profile is restricted to that surface which extends downwind beyond the transition distance.

TABLE 4

VALUES OF δ AND V_*

CALCULATED FROM THE EXPERIMENTAL DATA

FOR PEGS

u_a = 30 ft/sec				$Z_o = 2.2 \times 10^{-2}$ in.			
x ft	10	20	30	40	50	60	70
x' ft	-30	-20	-10	0	10	20	30
δ in.	3.07	4.29	5.97	7.59	9.00	10.38	12.10
V_* ft/sec	2.32	2.23	2.11	2.01	1.97	1.91	1.89

The velocity profile over a rough surface of small elements is expressed by

$$\frac{u - u_a}{V_*} = A \log \frac{Z}{\delta} + B \quad . \tag{4.1}$$

The velocity profile modified by the momentum absorption of tall simulated plants may be expressed by

$$\frac{u - u_a}{V_*} = A \log \frac{Z}{\delta} + B - \frac{\Delta u}{V_*} \quad . \tag{4.2}$$

The last term $\frac{\Delta u}{V_*}$ on the right hand side of Equation (3.28) represents the net effect of the tall plant surface. Therefore, it ought to be expressed in terms of such parameters as the height, spacing, and slope of the roughness elements.

An evaluation of $\frac{\Delta u}{V_*}$ was performed using each set of experimental data, and the results are shown in Figs. 4-10 and 4-11. These figures indicate that part of the velocity's maximum net diminution is caused by the simulated vegetation at $Z/\delta = 0.2$. The width, defined by $\frac{\Delta u}{V_*}$ becoming zero in the upper flow, is used to plot a normalization curve. The normalized data are found in Fig. 4-12. Similar results may be obtained by applying an equation applicable to the wake behind a symmetrical cylinder,

$$\frac{\Delta u}{(\Delta u)_{max}} = \left\{ 1 - \frac{\eta'}{\eta_o}^{3/2} \right\}^2 \quad , \tag{4.3}$$

where $\eta' = \eta - 0.2$ and $\eta' = \eta_o$ at the edge of the wake.

On the basis of the agreement between experimental data and Equation (4.3), it is suggested that $\frac{\Delta u}{V_*}$ can be expressed as

$$\frac{\Delta u}{V_*} = \left(\frac{\Delta u}{V_*} \right)_{max} \left(1 - \xi^{3/2} \right)^2 , \qquad (4.4)$$

where $\xi = \eta'/\eta_o$. It should be noted that $\left(\frac{\Delta u}{V_*} \right)_{max}$ and η_o might be a function of the height, shape, spacing, and mean velocity as can be seen in Fig. 4-10 and 4-11. However, there are not enough data to determine a functional relationship. η_o is almost too large a value to support the theory that the above height is of the same order as the height of the tall elements.

An exponential velocity profile within plants may be applicable to the upper portions of vegetative canopies. The exponential profile of Inoue (1963) is indicated by the dotted line in Fig. 4-12.

On the basis of the preceding discussion, the velocity distribution in and above vegetative canopies is expressed by

$$\frac{u - u_a}{V_*} = A \log \eta + B - \left(\frac{\Delta u}{V_*} \right)_{max} \left(1 - \xi^{3/2} \right)^2 + \alpha , \qquad (4.5)$$

where α is defined by $u - u_a$ becoming zero at $\eta - 0.2 = \eta_o$.

Thus, α is given by

$$\alpha = - A \log (\eta_o + 0.2) - B . \qquad (4.6)$$

Therefore, Equation (4.5) can be expressed by

$$\frac{u - u_a}{V_*} = A \log \eta - \left(\frac{\Delta u}{V_*} \right)_{max} \left(1 - \xi^{3/2} \right)^2 - \alpha' , \qquad (4.7)$$

where $\alpha' = A \log (\eta_o + 0.2)$.

Equation (4.7) may be written as

$$\frac{u - u_a}{V_*} = A \log \left(\frac{\eta}{\eta_o + 0.2} \right) - \left(\frac{\Delta u}{V_*} \right)_{max} (1 - \xi^{3/2})^2 \quad \cdot (4.8)$$

Upon making the substitutions $Z_1 = \eta_o \delta$ and $Z_2 = 0.2\,\delta$, Equation (4.8) becomes

$$\frac{u - u_a}{V_*} = A \log \left(\frac{Z}{Z_1 + Z_2} \right) - \left(\frac{\Delta u}{V_*} \right)_{max} \left\{ 1 - \left(\frac{Z - Z_2}{Z_1} \right)^{3/2} \right\}^2 . \quad (4.9)$$

The quantities Z_1 and Z_2 are a function of distance downwind from the leading edge of a tall, rough surface.

Chapter V

VERTICAL VELOCITIES IN AND ABOVE VEGETATIVE CANOPIES

In the preceding discussion an equation was obtained for the mean velocity profile in and above tall simulated vegetation. In the discussion that follows, the subscripts 1 and 2 will refer to boundary-layer profiles associated with rough surfaces consisting of tall and small elements, respectively.

Equation (4.7) may be used to define a stream function,

$$- f'(\eta) = A \log \eta - \left(\frac{\Delta u}{V_*} \right)_{max} (1 - \xi^{3/2})^2 - \alpha' = \frac{u_1 - u_a}{V_*} \quad . \tag{5.1}$$

The stream function $f(\eta)$ is obtained by integrating Equation (5.1),

$$- f(\eta) = A (\eta \log \eta - \eta) - \eta_o \left(\frac{\Delta u}{V_*} \right)_{max} \int (1 - \xi^{3/2})^2 \, d\xi - \alpha' \eta + \beta \quad , \tag{5.2}$$

where β is defined by $f(0) = 0$.

Equation (3.5) is still satisfactory for a general vertical velocity. Thus, a dimensionless vertical velocity in and above a plant cover area is given by:

$$\frac{w_1}{V_*}\frac{1}{\frac{d\delta}{dx}} = \left\{ f(\eta) - \eta f'(\eta) \right\}$$

$$= \eta \left\{ A + \left(\frac{\Delta u}{V_*} \right)_{max} \left(1 - \frac{4}{5}\xi^{3/2} + \frac{1}{4}\xi^3\right) - \right.$$

$$\left. - \left(\frac{\Delta u}{V_*} \right)_{max} \left(1 - \xi^{3/2}\right)^2 \right\} \quad . \tag{5.3}$$

On the other hand, the velocity profile for a rough surface of small elements may also be used to define a stream function;

$$- f'(\eta) = A \log \eta + B = \frac{u_2 - u_a}{V_*}$$

$$- f(\eta) = A (\eta \log \eta - \eta) + B\eta \quad . \tag{5.4}$$

Therefore, the vertical velocity over a rough surface of small elements is given by

$$\frac{w_2}{V_*}\frac{1}{\frac{d\delta}{dx}} = \eta A \quad . \tag{5.5}$$

Equation (5.5) shows that the vertical velocity increases with height. The ratio of the vertical flow caused by tall elements to that caused by small elements can be expressed as

$$\frac{w_1}{w_2} = \left\{ 1 + \frac{\left(\frac{\Delta u}{V_*} \right)_{max}}{A} \left(\frac{6}{5}\xi^{3/2} - \frac{3}{4}\xi^3 \right) \right\} \quad . \tag{5.6}$$

As an example, Equation (5.6) was evaluated when the flexible strips were subjected to an ambient velocity of 20 ft/sec. The results of this calculation are shown in Fig. 5-1. Note that $\frac{du}{dx}$ becomes larger at the outer layer of the flow over the vegetation area. This

fact is in agreement with the two-dimensional continuity equation. Raw data, seen in Figs. 4-3, 4-4, and 4-5, also reveal this same situation. Fig. 5-1 indicates that the dimensionless simulated vegetation height is h_e/δ, provided that the deflected height is taken as the reference height h_e. The deflected height is 3.9 inches for an ambient velocity of 20 fps (see Plate 1965).

Figure 5-2 depicts the change in velocity profiles associated with flow over a rough surface consisting of tall elements. The data contained in this report indicate that the variation of the mean wind velocity with distance downwind from leading edge of a tall simulated vegetative area, can be predicted by the wake-theory.

Chapter VI

CONCLUSION

In the preceding sections the authors have investigated a universal velocity distribution in and above an area covered with vegetation. This study indicates that such a distribution can be expressed in terms of two significant parameters--the maximum net diminution velocity and the apparent wake edge created by tall vegetation. These parameters depend upon the shape, height, and spacing of the roughness elements. The results mentioned above, however, must be supported by additional experimental data. These data will be obtained in further explorations of the phenomena produced by various types of plants. Once these data are accumulated, investigators will be able to focus their attention on other exchange processes such as evaporation from a vegetative surface.

REFERENCES

REFERENCES

Batchelor, G. K., (1964): Diffusion from Sources in a Turbulent Boundary Layer. Polska Akademia Nauk, Instytut Podstdwowych Problemow Techniki Archives de Mecanique Appliquee, 3, XVI, Warszawa.

Cermak, J. E., (1963): Lagrangian Similarity Hypothesis Applied to Diffusion in Turbulent Shear Flow. Journal of Fluid Mechanics, Vol. 15, Part I.

Cermak, J. E., and E. J. Plate, (1963): Investigation to Develop Wind Tunnel Technique for Measuring Atmospheric Gaseous Diffusion in Model Vegetative Surfaces. Final Report on Contract No. 12-14-100-4546 (41) with U.S. Department of Agriculture, Agriculture Research Service, Soil and Water Conservation Research Division, Beltsville, Maryland. CER63.

Cionco, R. M., W. D. Ohmstede, and J. F. Appleby, (1963): Model for Wind Flow in an Idealized Vegetative Canopy. Meteorological Research Note No. 5, Meteor. Dept., U.S. Army Electr. Res. and Dev. Activity, Fort Huachuca, Arizona, 35.

Clauser, F. H., (1954): The Turbulent Boundary Layer. Department of Aeronautics, The Johns Hopkins University.

Goldstein, S. (ed.), (1965): Modern Developments in Fluid Dynamics. Dover Publication, Inc., New York.

Inoue, E., (1963): On the Turbulent Structure of Airflow Within Crop Canopies. Journal of Meteorological Society of Japan, Vol. 41, No. 6

Lemon, E. R., (ed.), (1963): The Energy Budget at the Earth's Surface, Part II. Production Research Report No. 2, Agric. Res. Service, U.S. Department of Agriculture.

Plate, E. J., and A. A. Quarishi, (1965): Modeling Velocity Distributions Inside and Above Tall Crops. Journal of Applied Meteorology, Vol. 4, No. 3.

Poreh, M. and J. E. Cermak, (1964): Study of Diffusion from a Line Source in a Turbulent Boundary Layer. International Journal of Heat and Mass Transfer, Vol. 7, pp. 1083-1095 Pergamon Press.

Tani, N., (1963): The Wind Over the Cultivated Field. The Bulletin of the National Institute of Agricultural Sciences. Series A, No. 10, March.

FIGURES

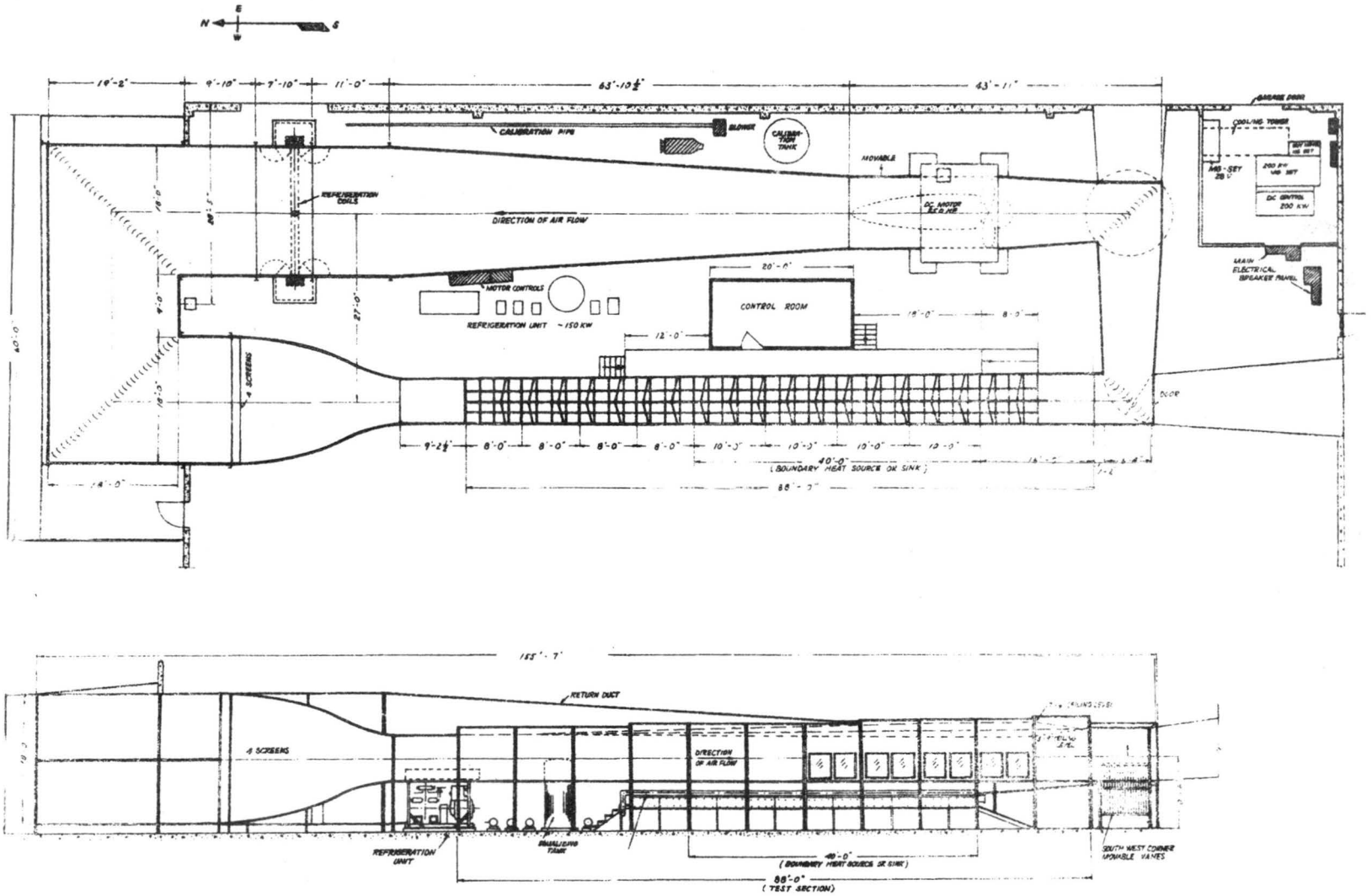

Fig. 1-1 Army Meteorological Wind Tunnel

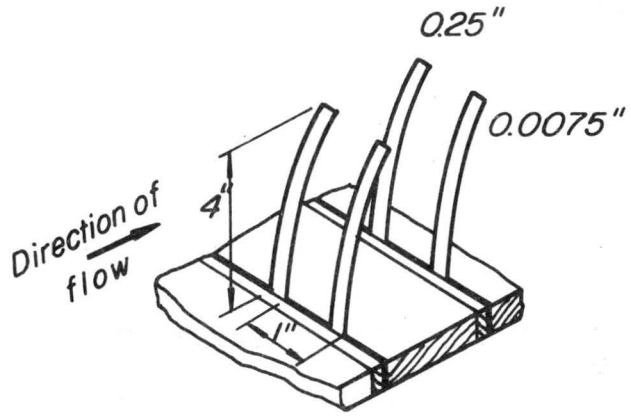

Figure 2-1 Rough surface of flexible plastic elements

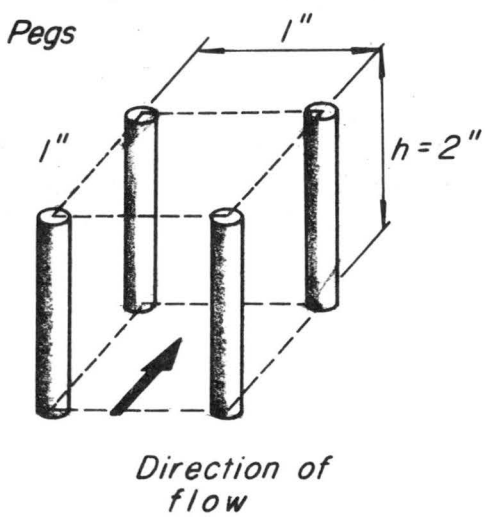

Figure 2-2 Rough surface of pegs

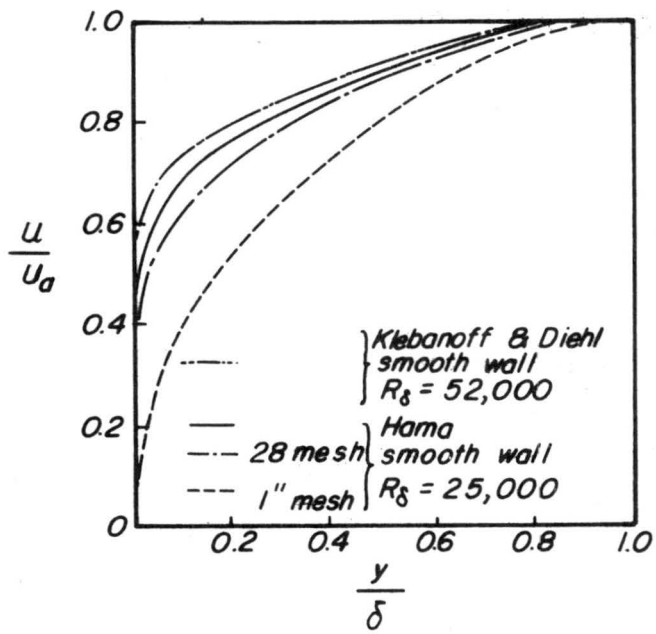

Figure 3-1 Turbulent boundary-layer profiles at constant pressure on smooth and rough walls (after Francis H. Clauser)

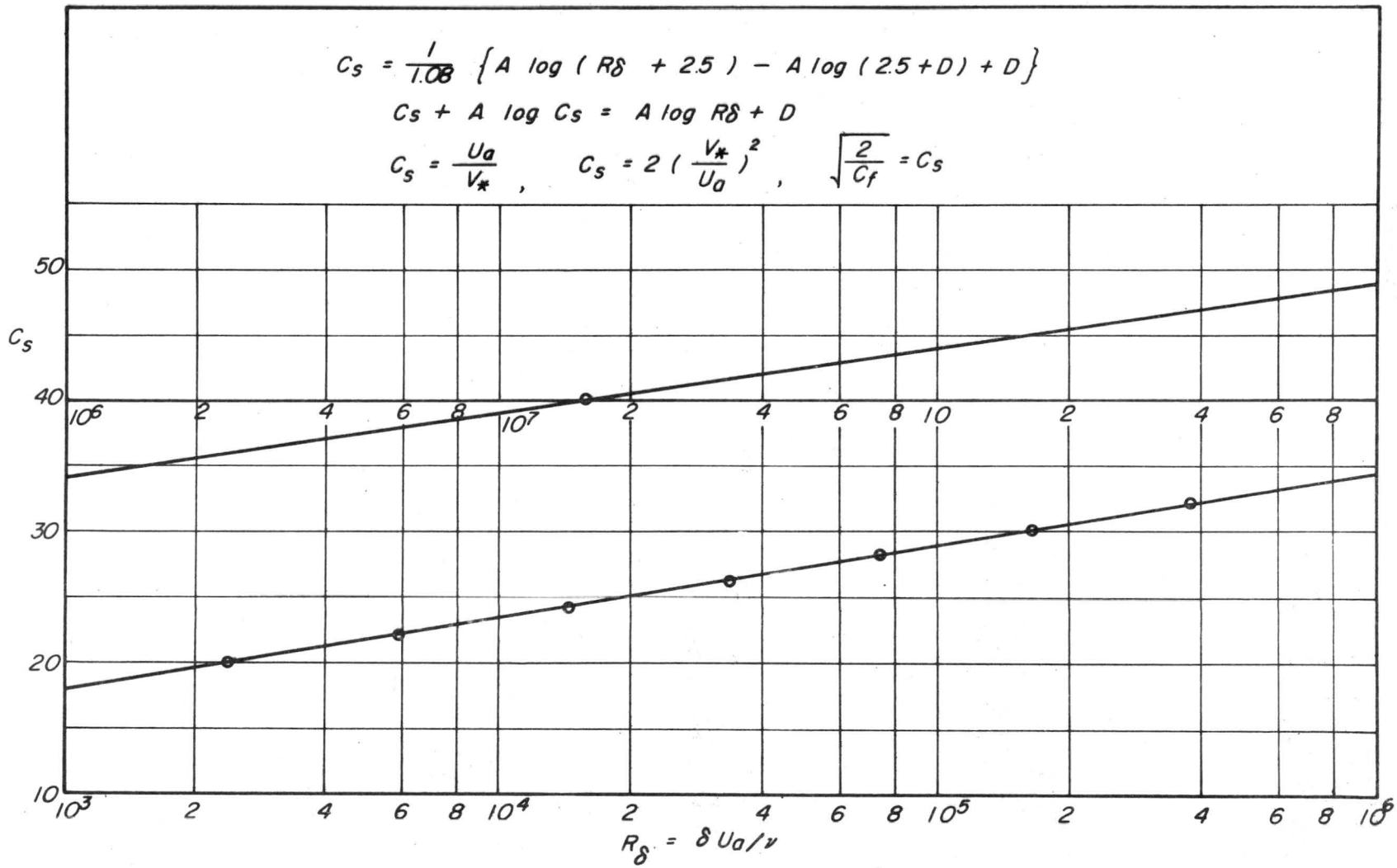

Figure 3-2 u_a/V_* vs. $\delta u/V$

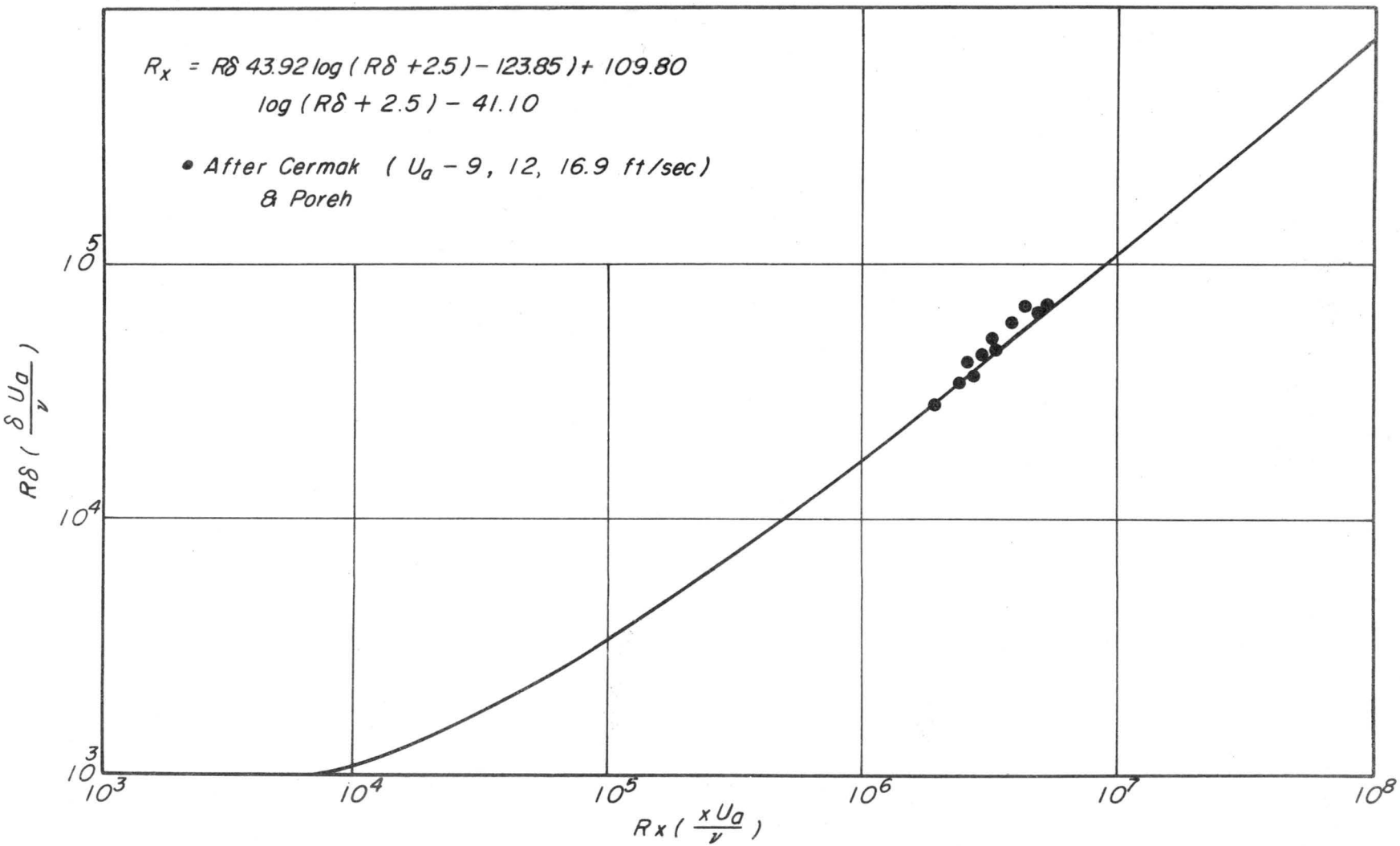

Figure 3-3 Variation of boundary-layer thickness for smooth plate

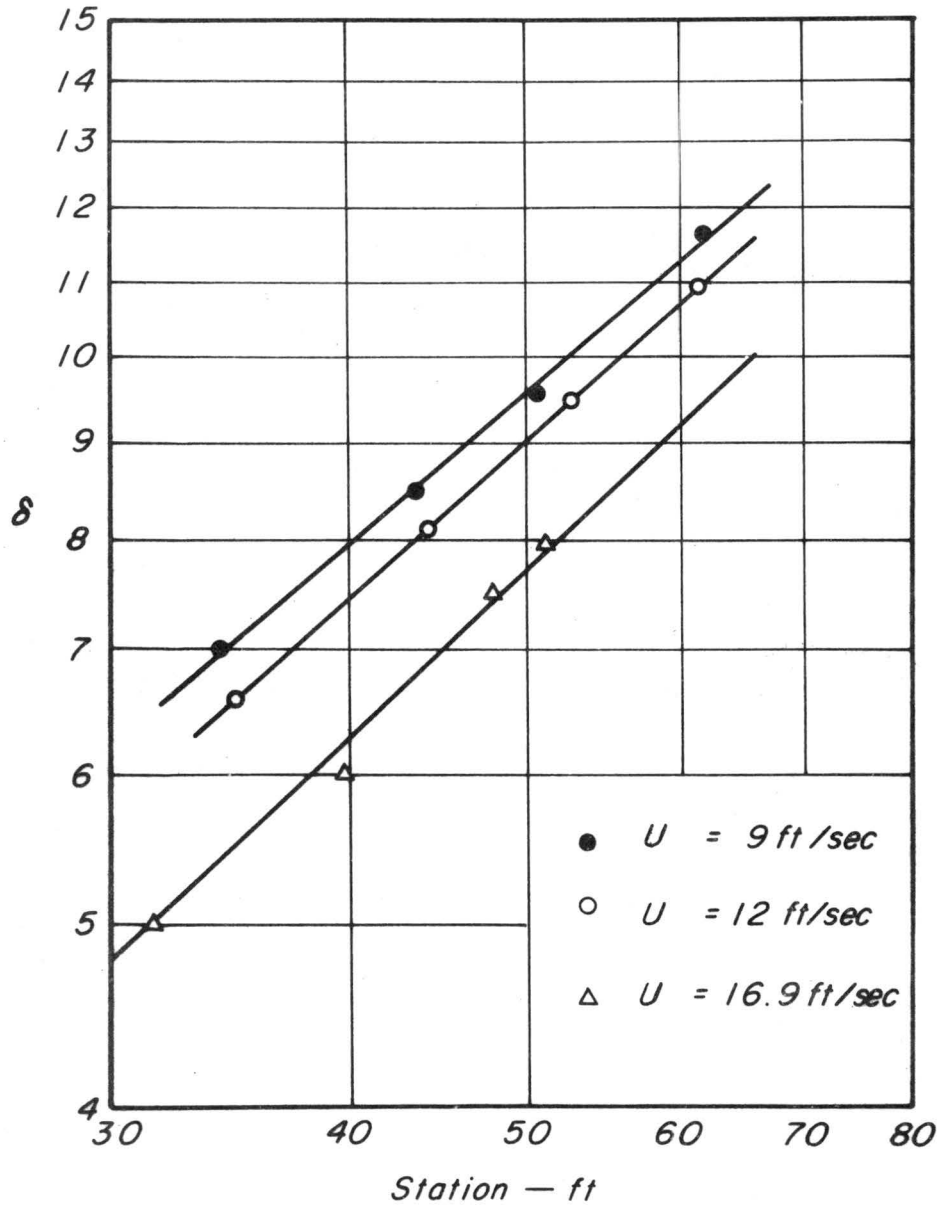

Figure 3-4 Variation of boundary-layer thickness (after Poreh and Cermak)

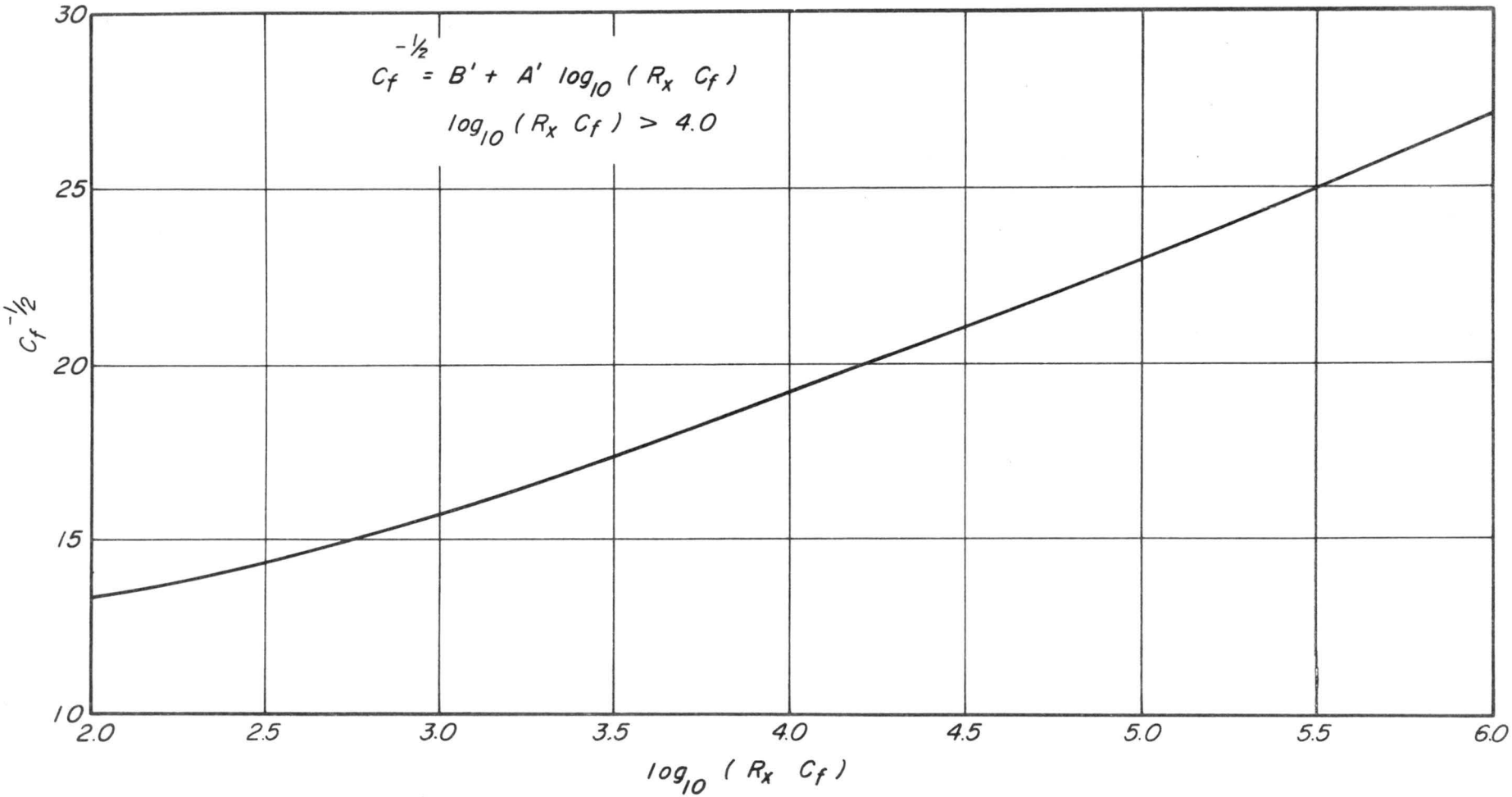

Figure 3-5 Local values of the skin-friction coefficient

C_f vs. $R_x C_f$

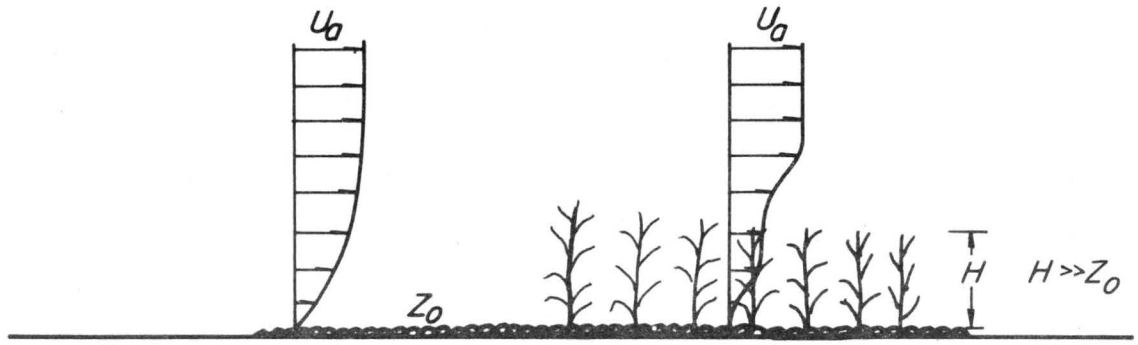

Figure 3-6 Schematical illustration of the fluid flow in the field

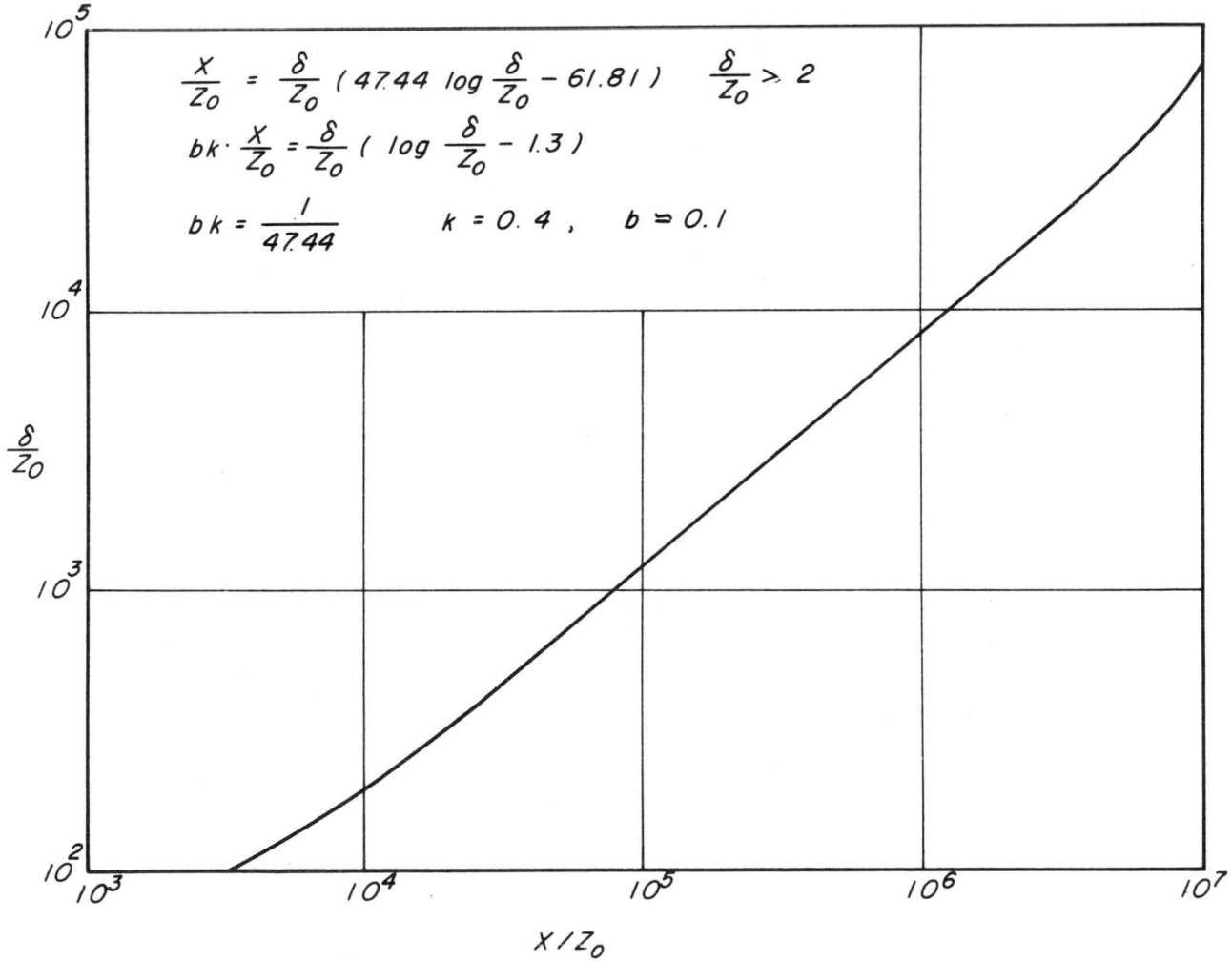

Figure 3-7 Variation of boundary-layer thickness for a rough plate consisting of small elements

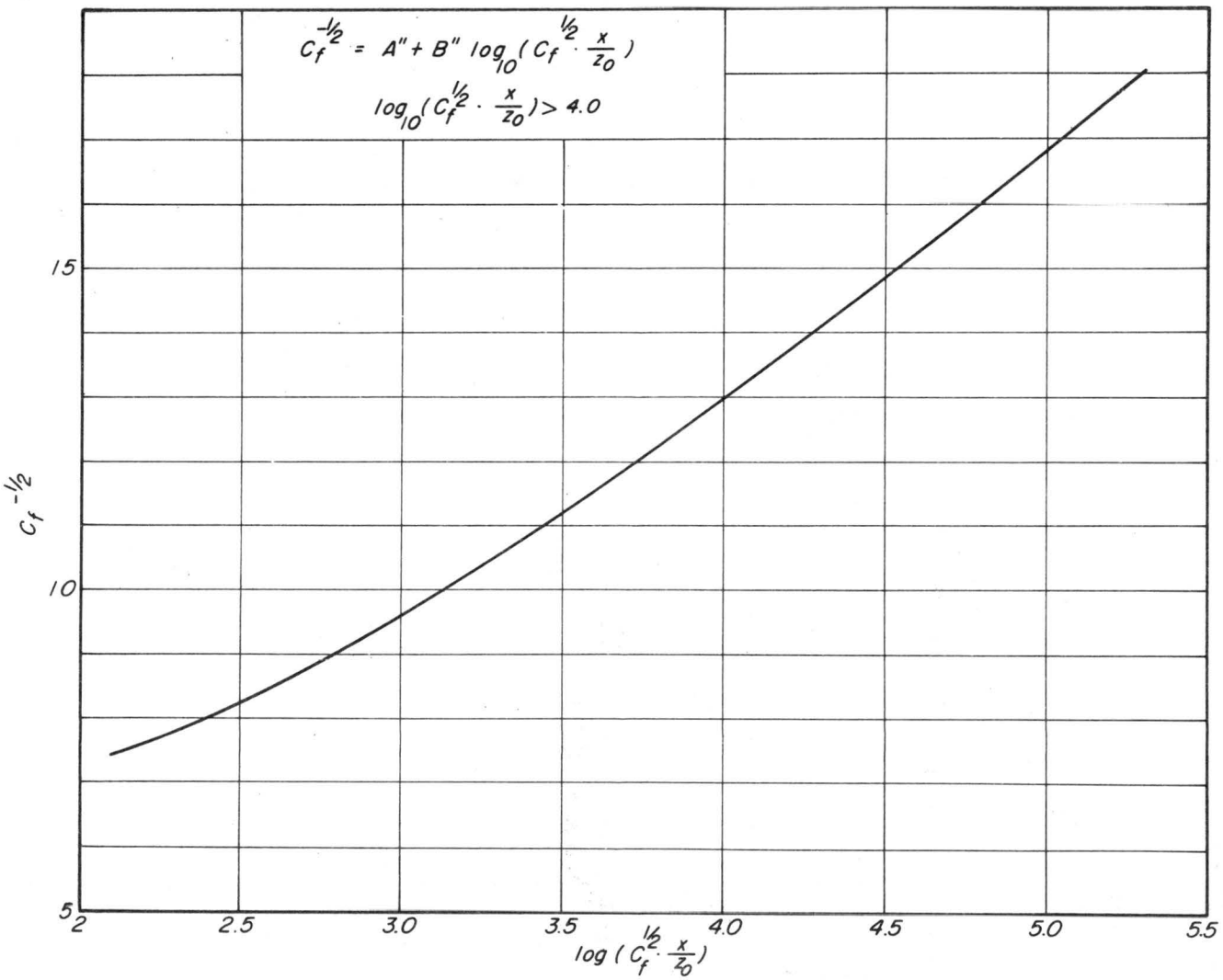

Figure 3-8 Local value of the skin-friction coefficient vs. a dimensionless downwind distance

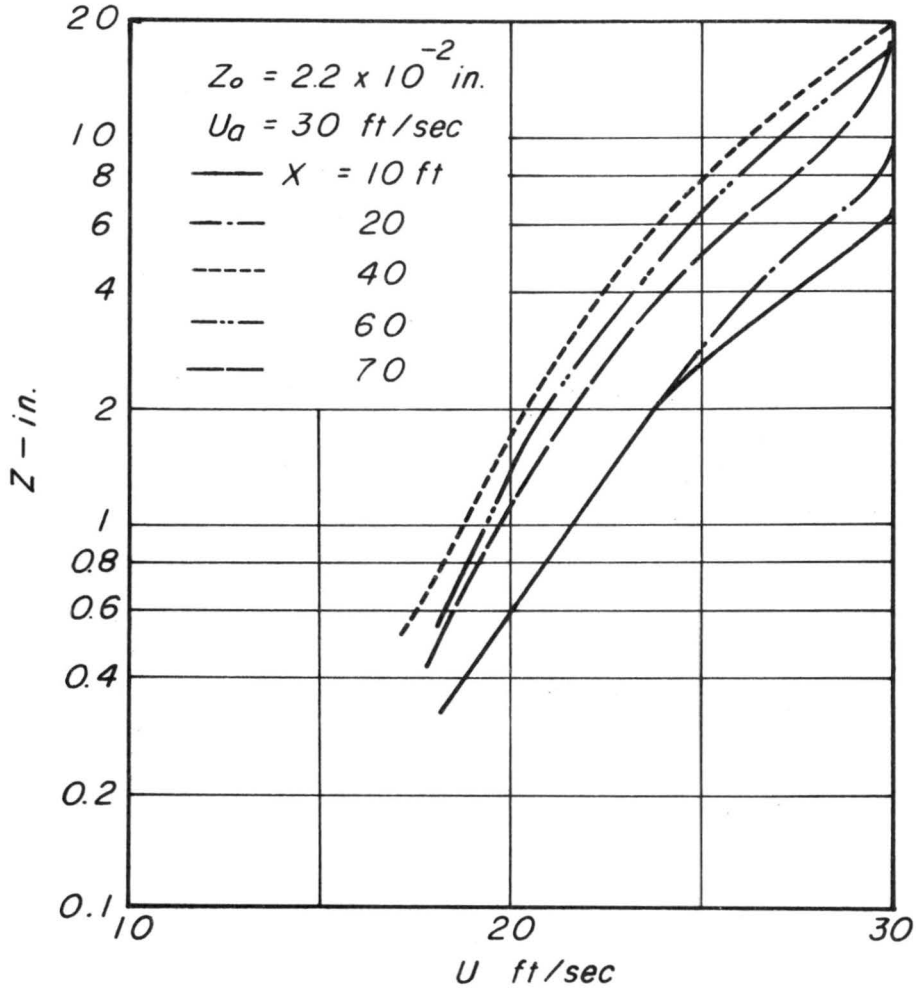

Figure 4-1 Velocity profiles at several distances from a leading edge

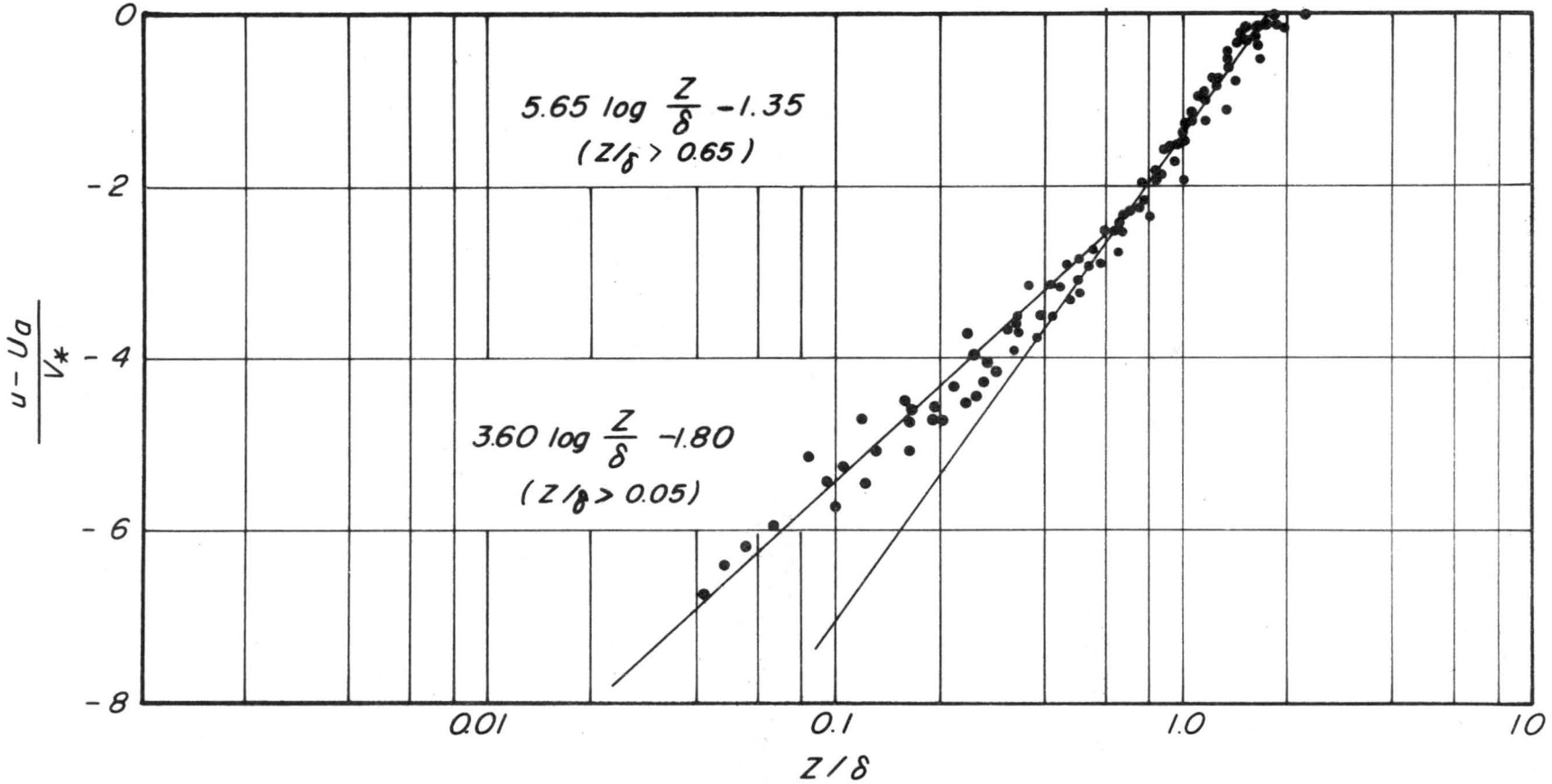

Figure 4-2 Logarithmic plot of universal profiles for turbulent boundary-layer at constant pressure

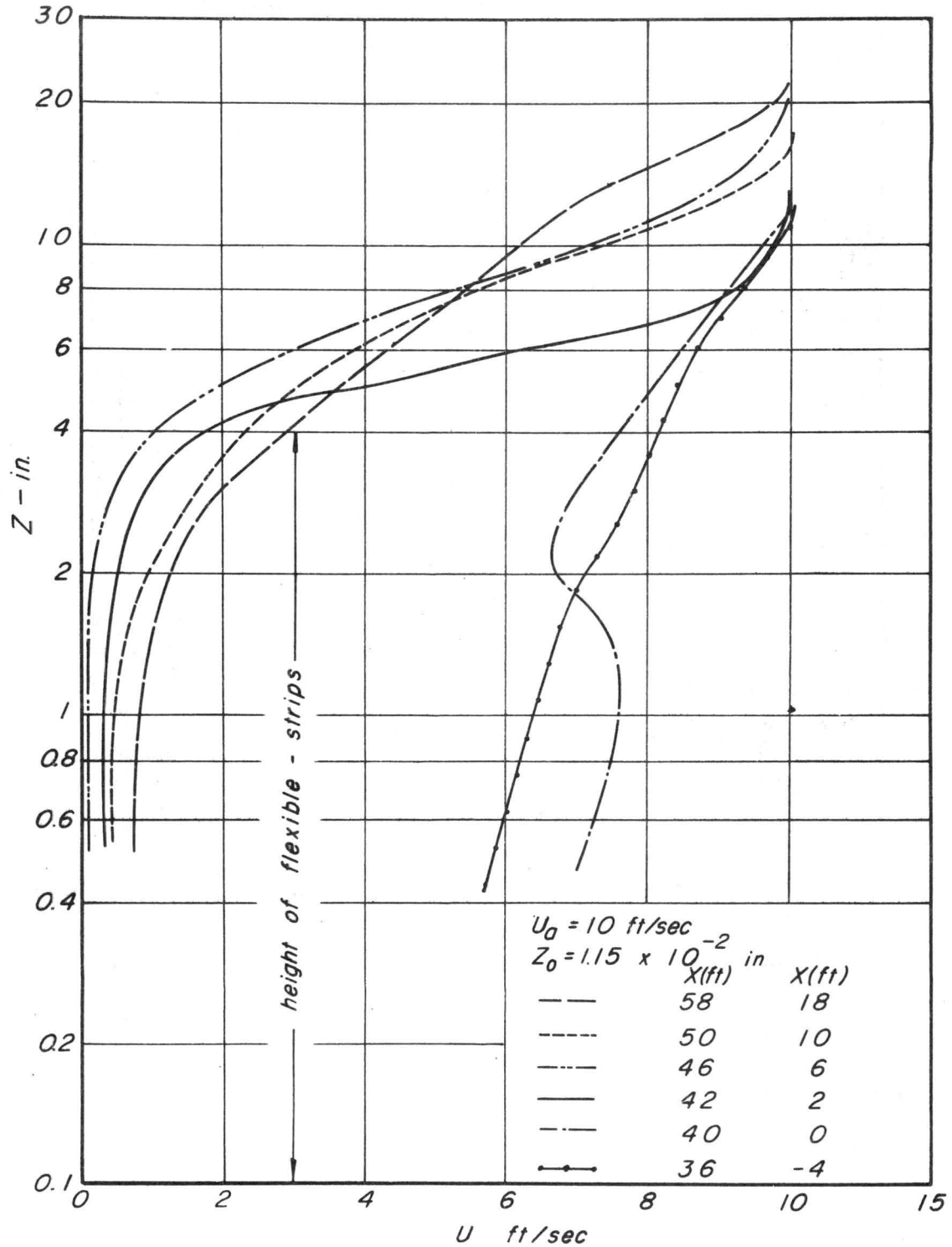

Figure 4-3 Velocity profiles in and above a rough surface of flexible plastic strips

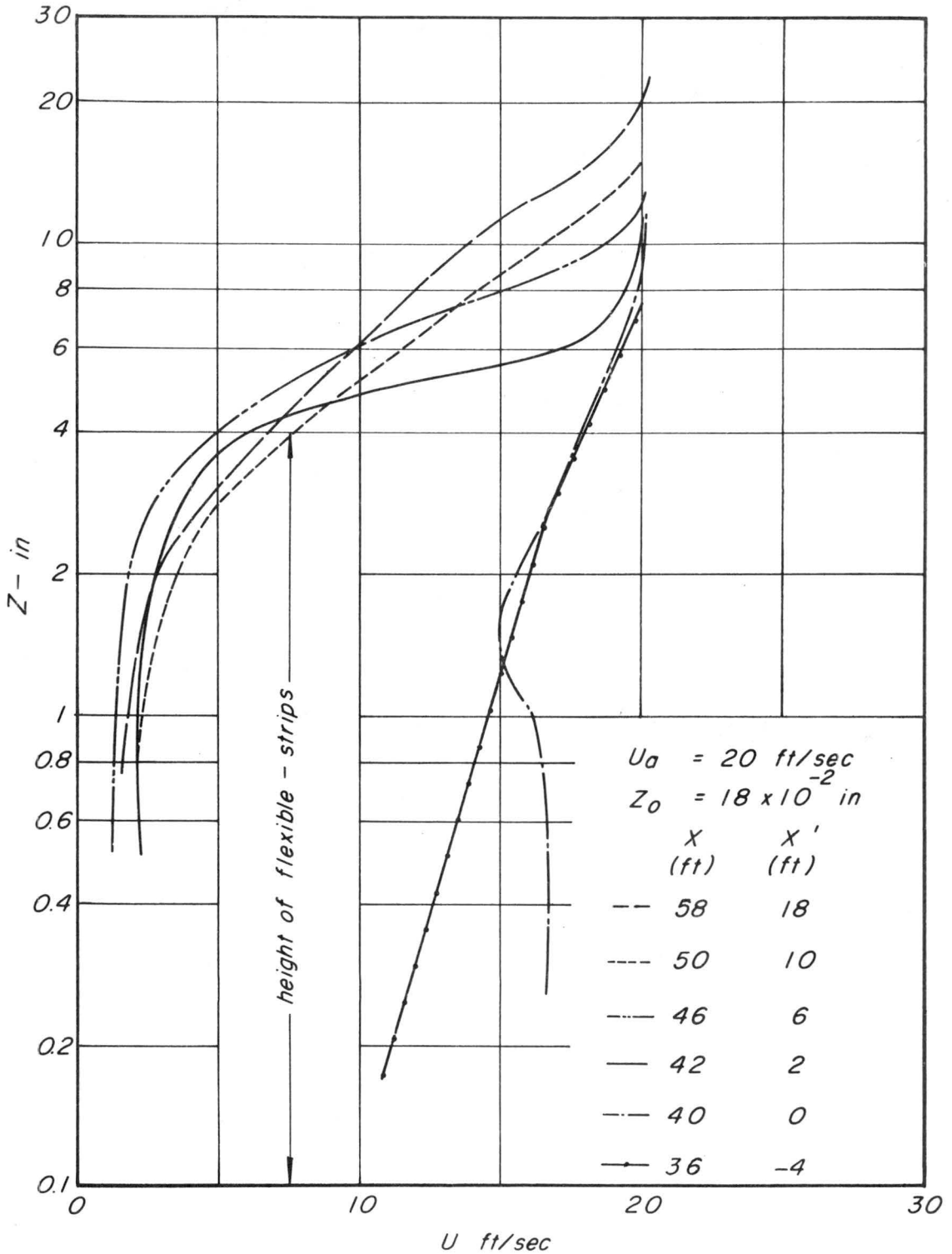

Figure 4-4 Velocity profiles in and above a rough surface of flexible plastic strips

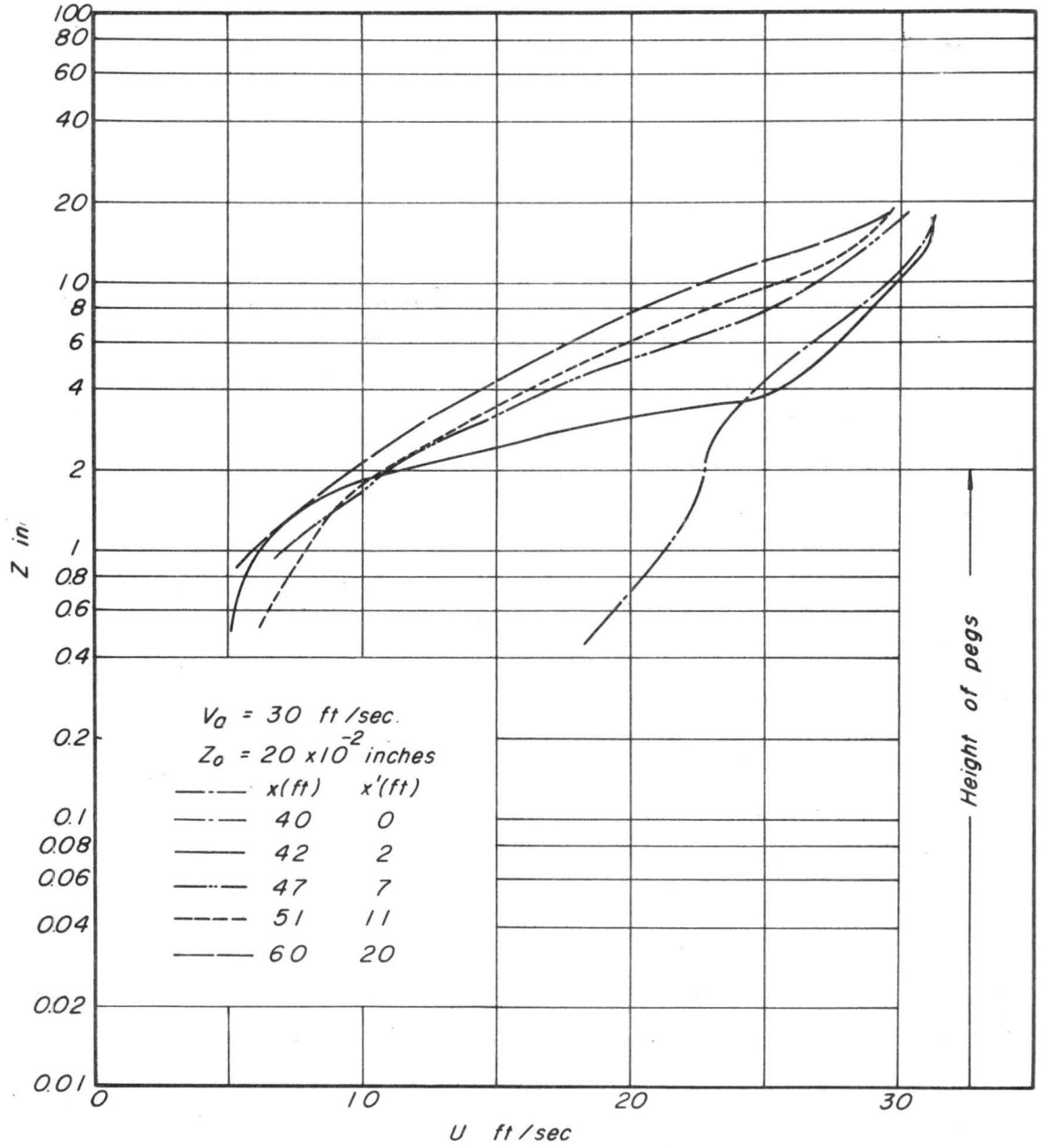

Figure 4-5 Velocity profiles in and above a rough surface of pegs

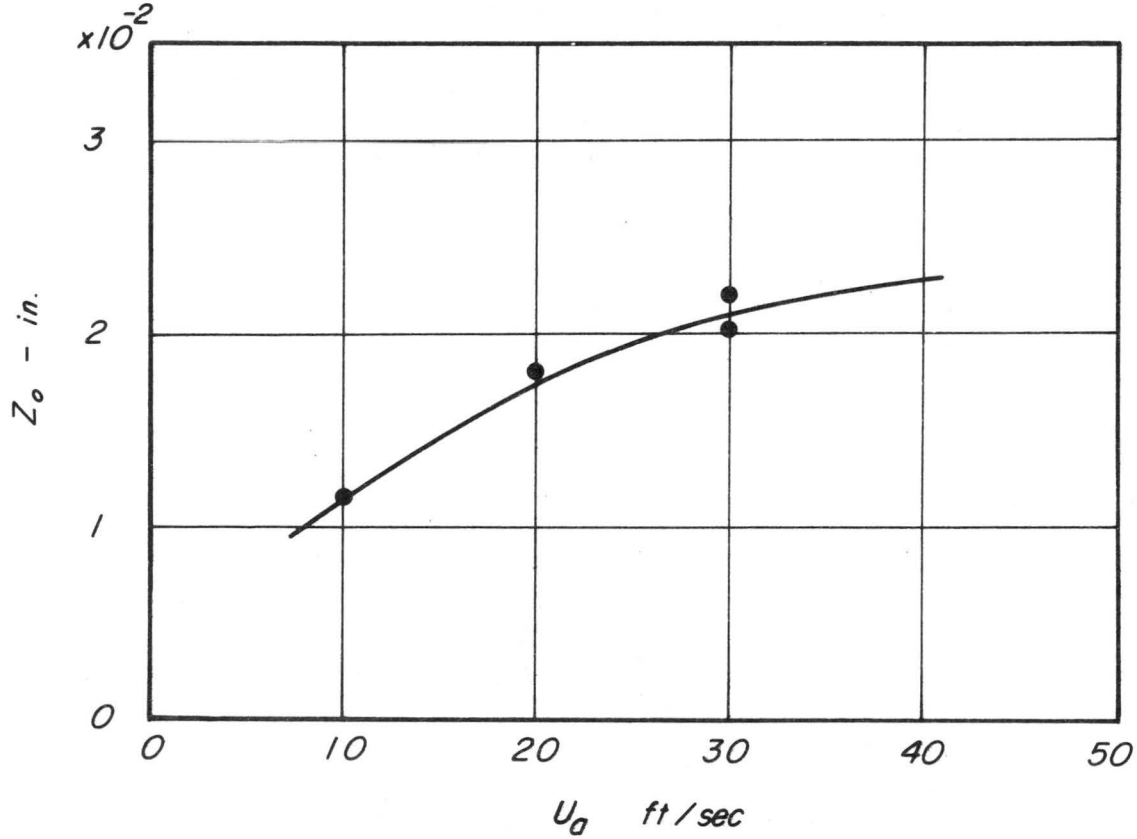

Figure 4-6 The relationship between roughness height Z_o and ambient velocity

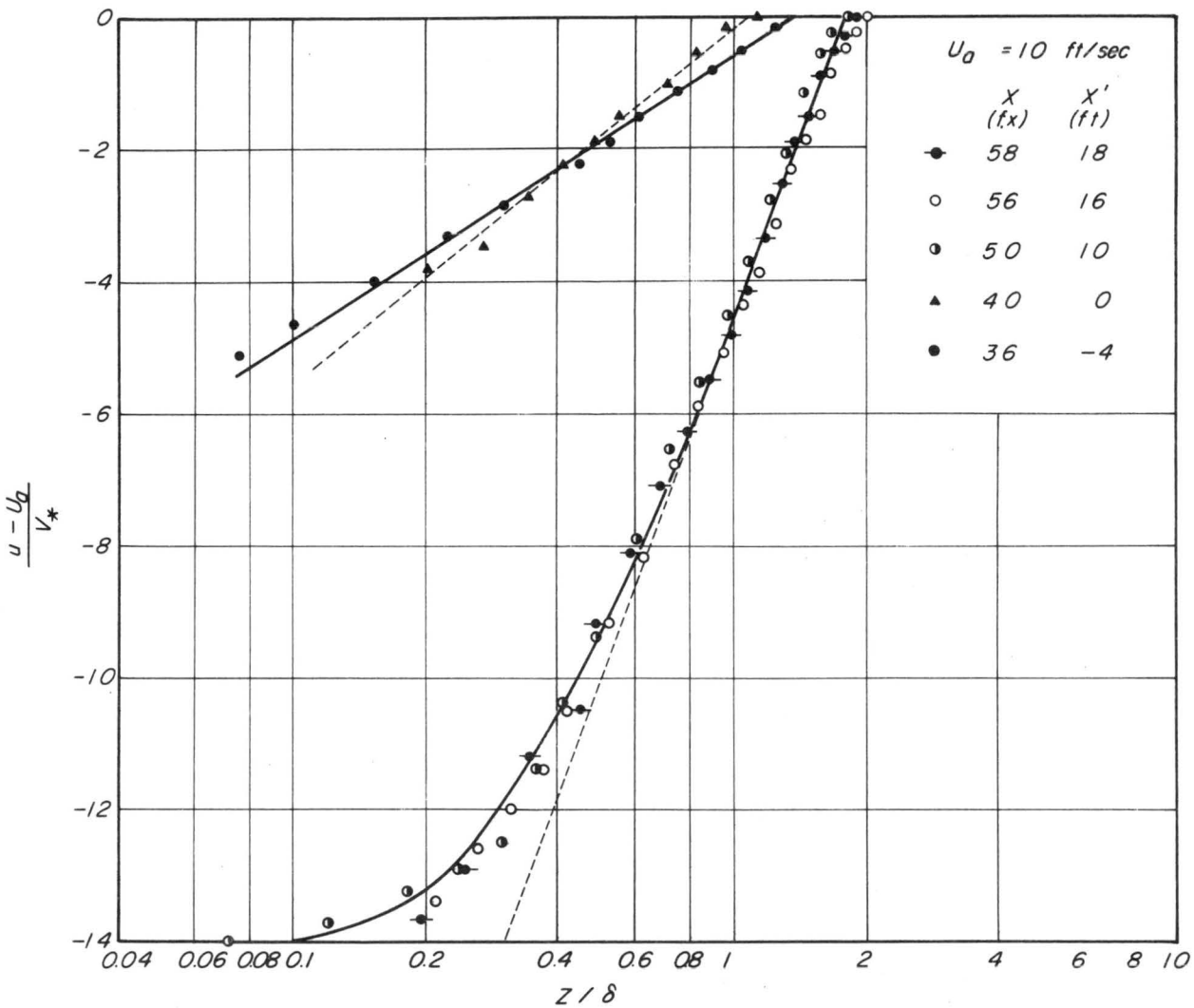

Figure 4-7 Logarithmic plot of universal velocity profile in and above the rough surface (plastic strips).

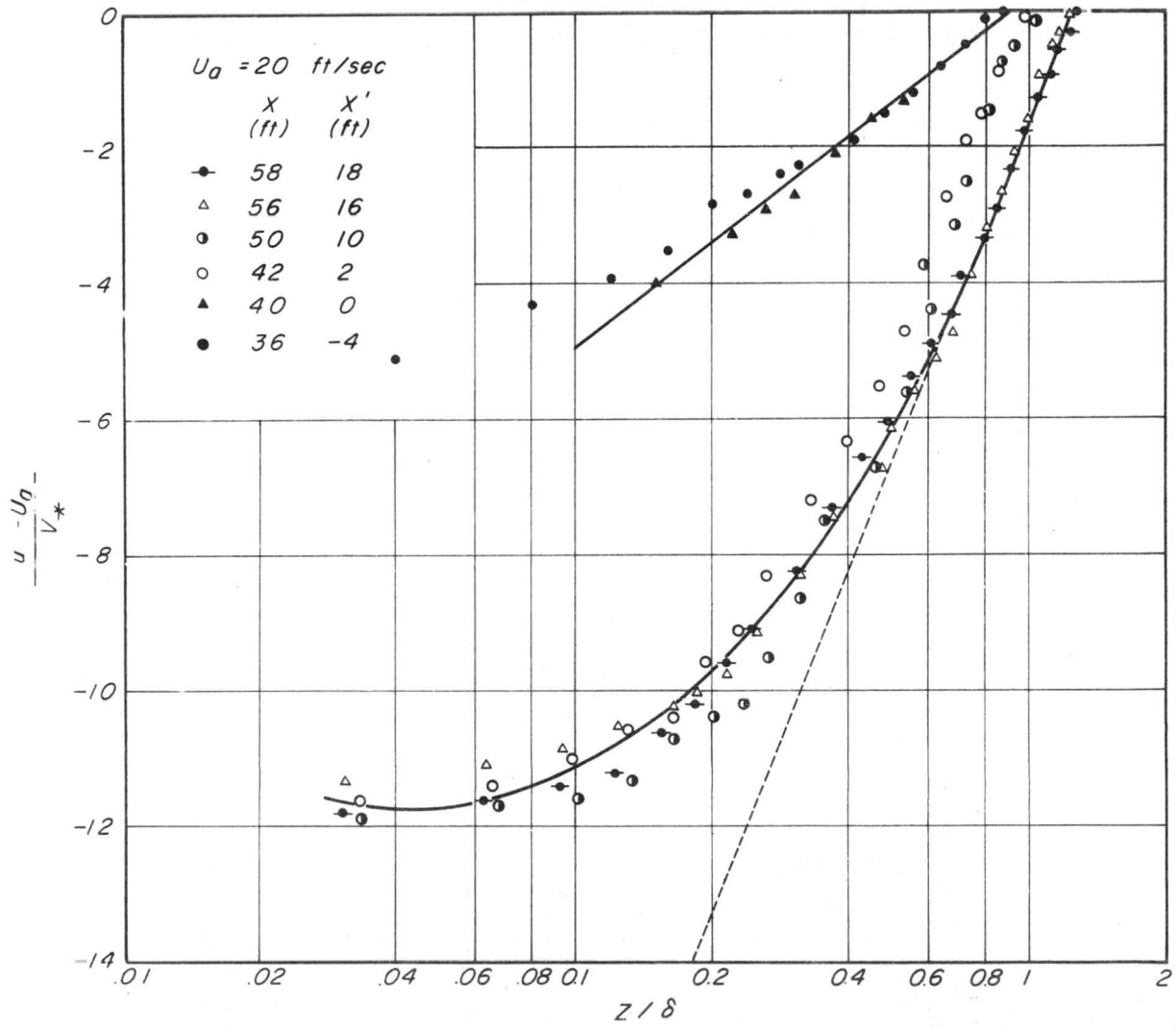

Figure 4-8 Logarithmic plot of universal profile in and above the rough surface (plastic strips).

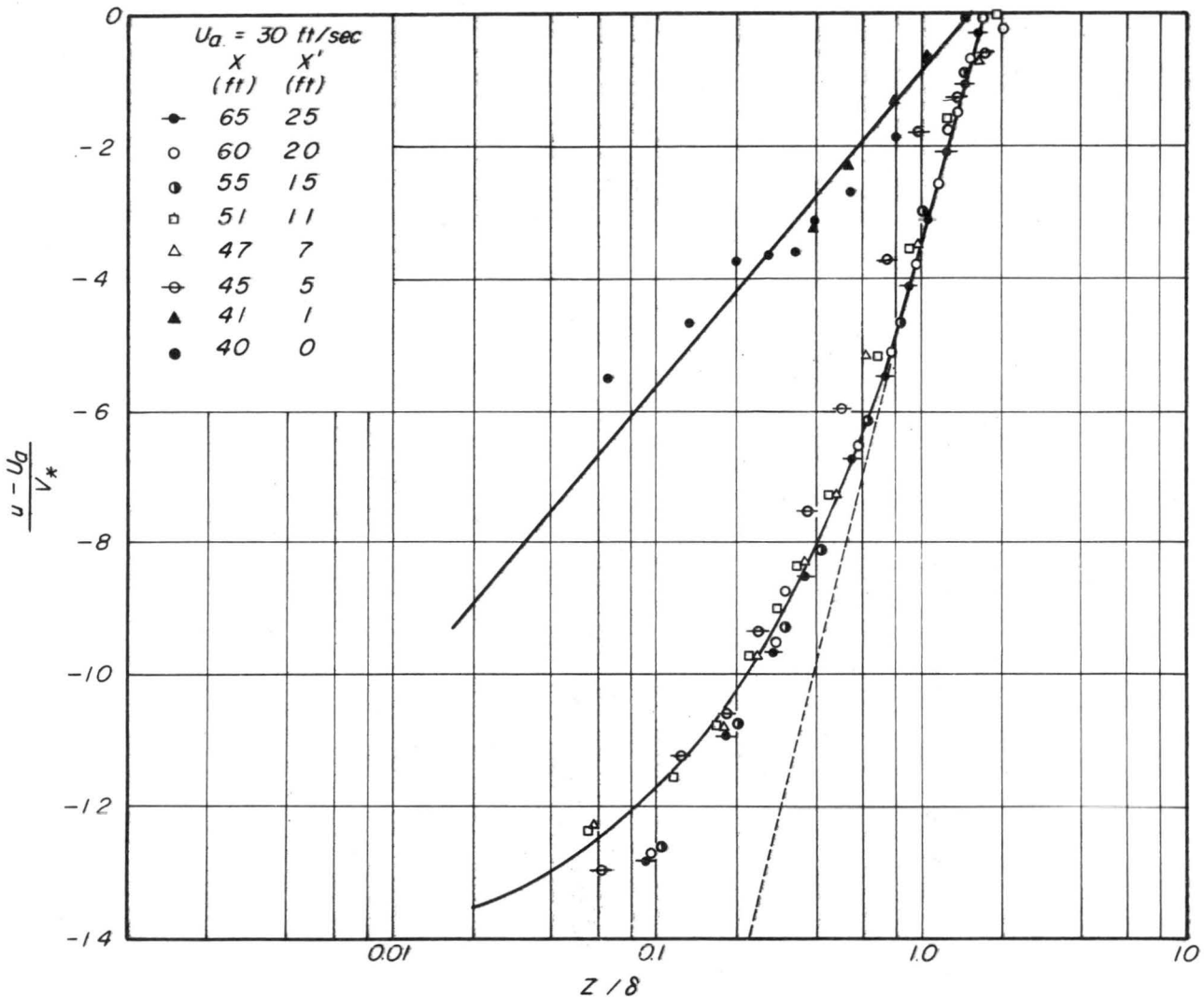

Figure 4-9 Logarithmic plot of universal profile in and above a rough surface (pegs).

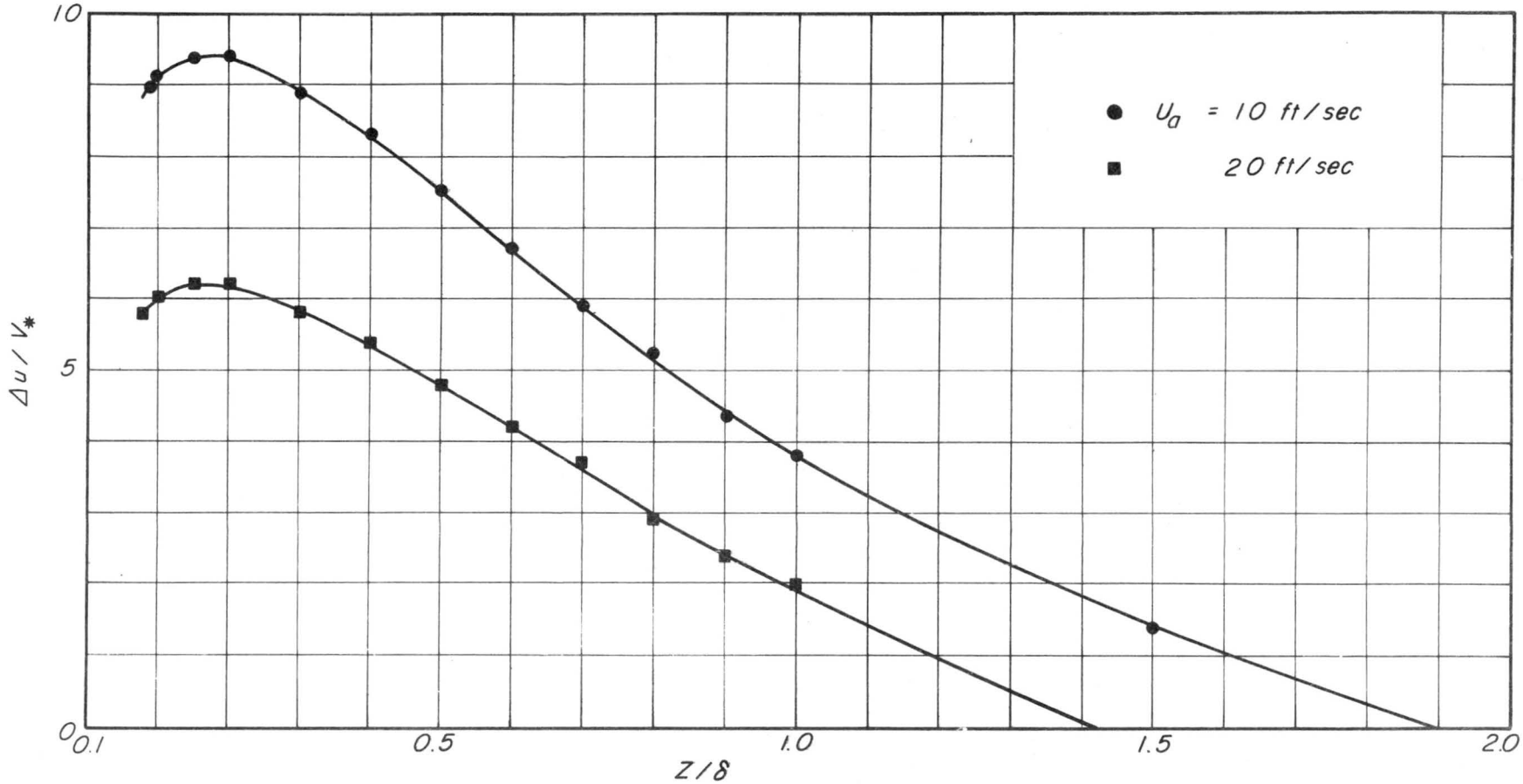

Figure 4-10 Wind velocity defect for logarithmic curve caused by a rough surface of flexible plastic strips

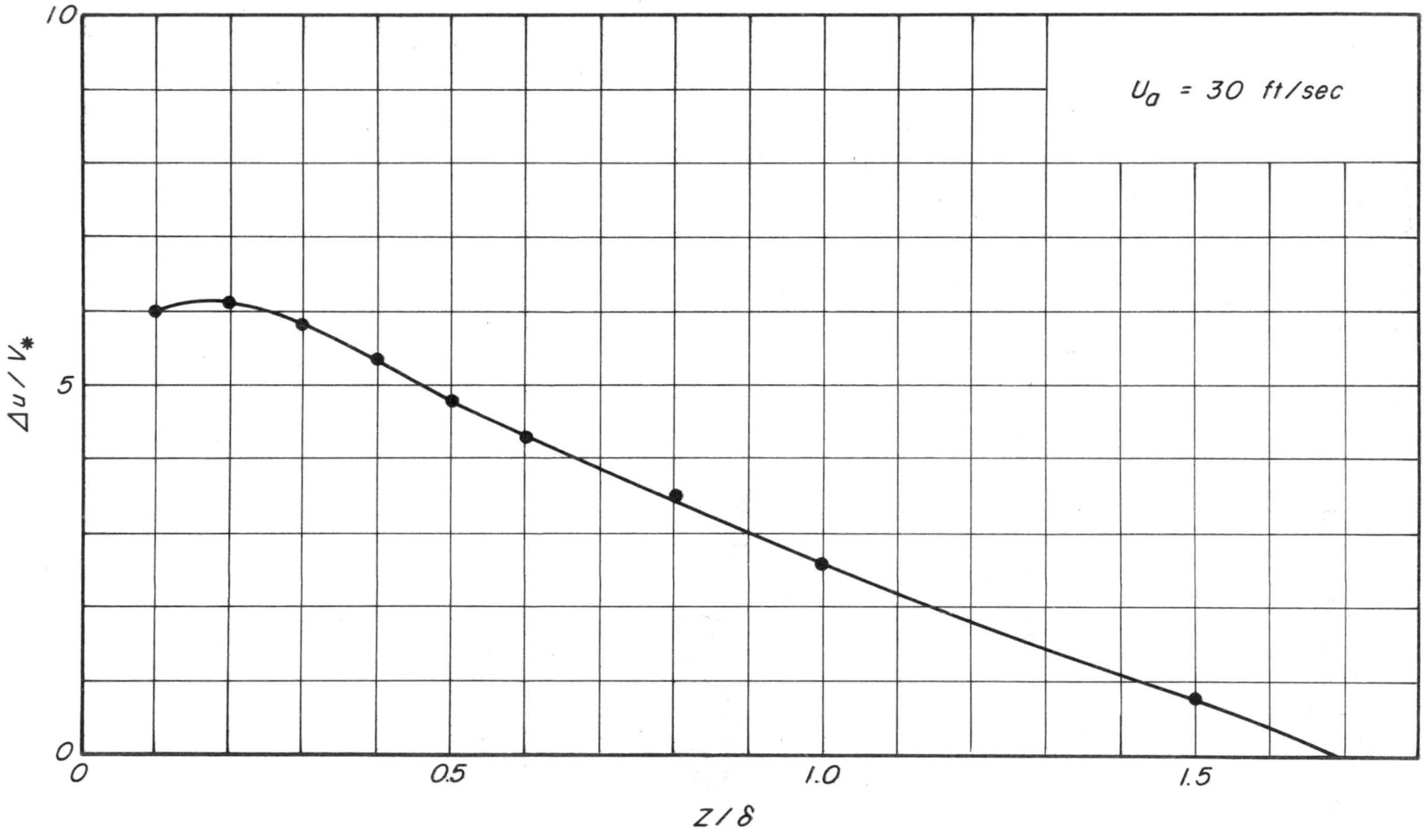

Figure 4-11 Wind velocity defect for logarithmic curve caused by a rough surface of pegs

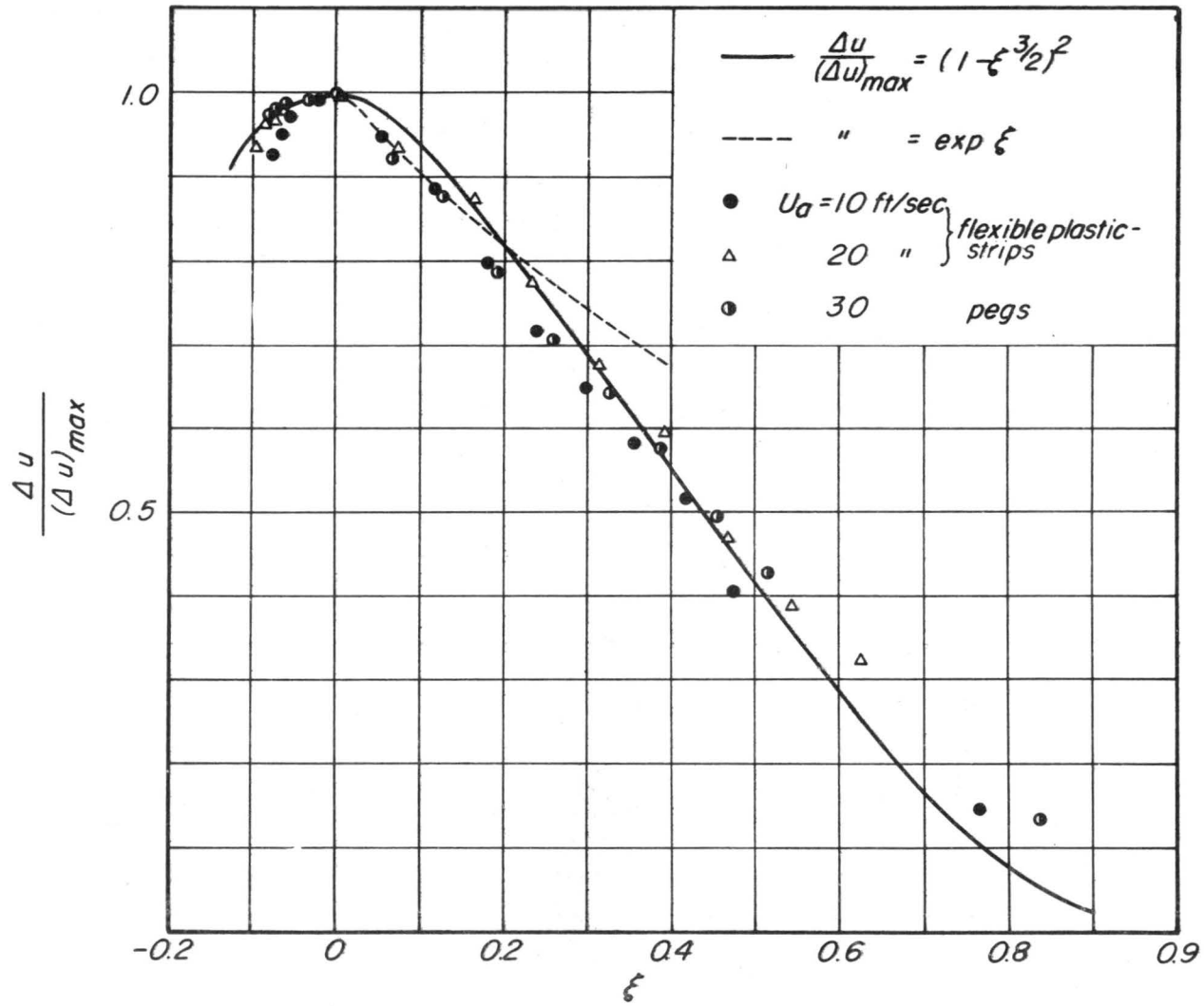

Figure 4-12 Normalized curve of the velocity defect caused by a rough surface of flexible plastic strips and pegs

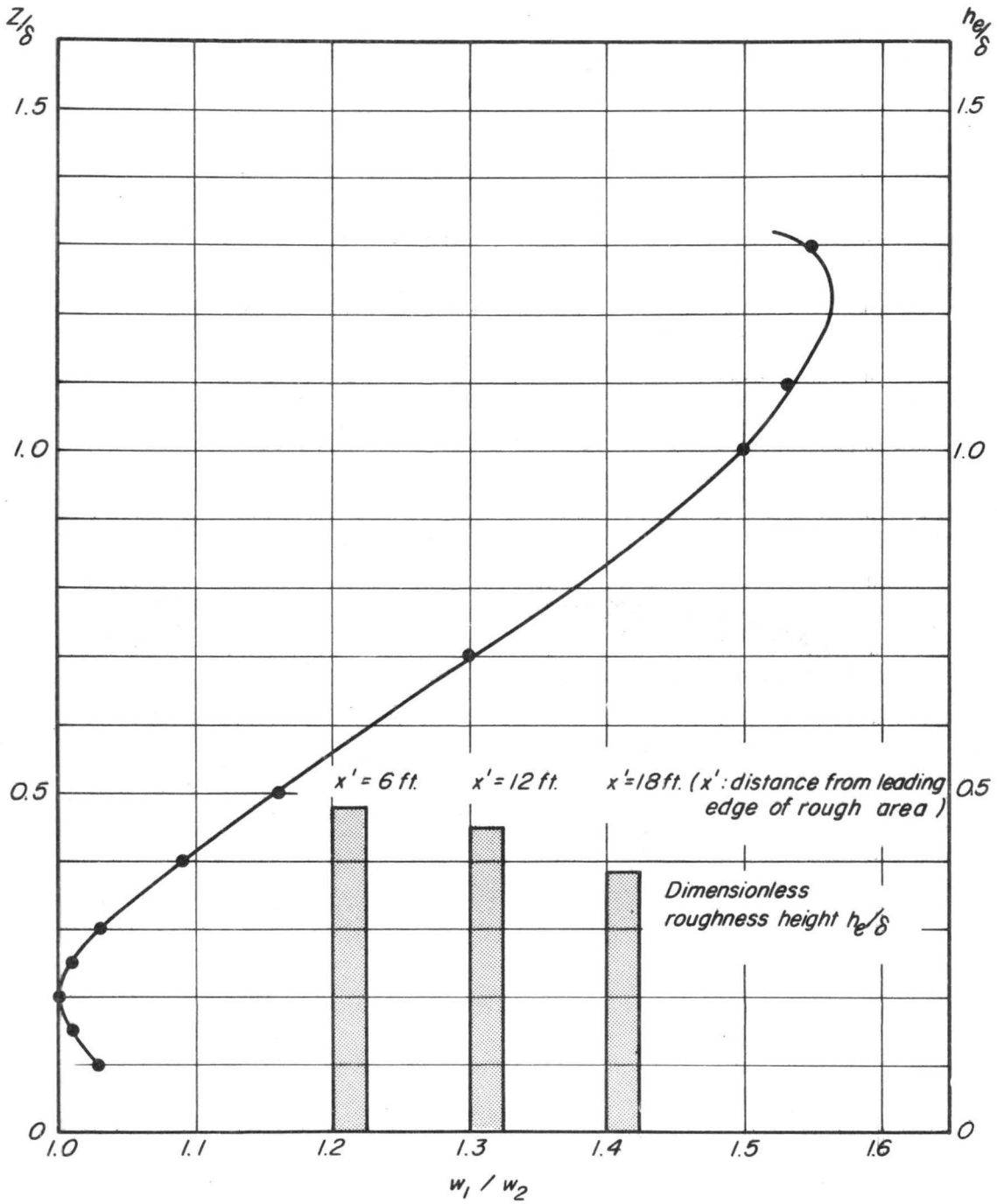

Figure 5-1 Ratio of vertical flow over a rough surface of tall elements to that for small elements

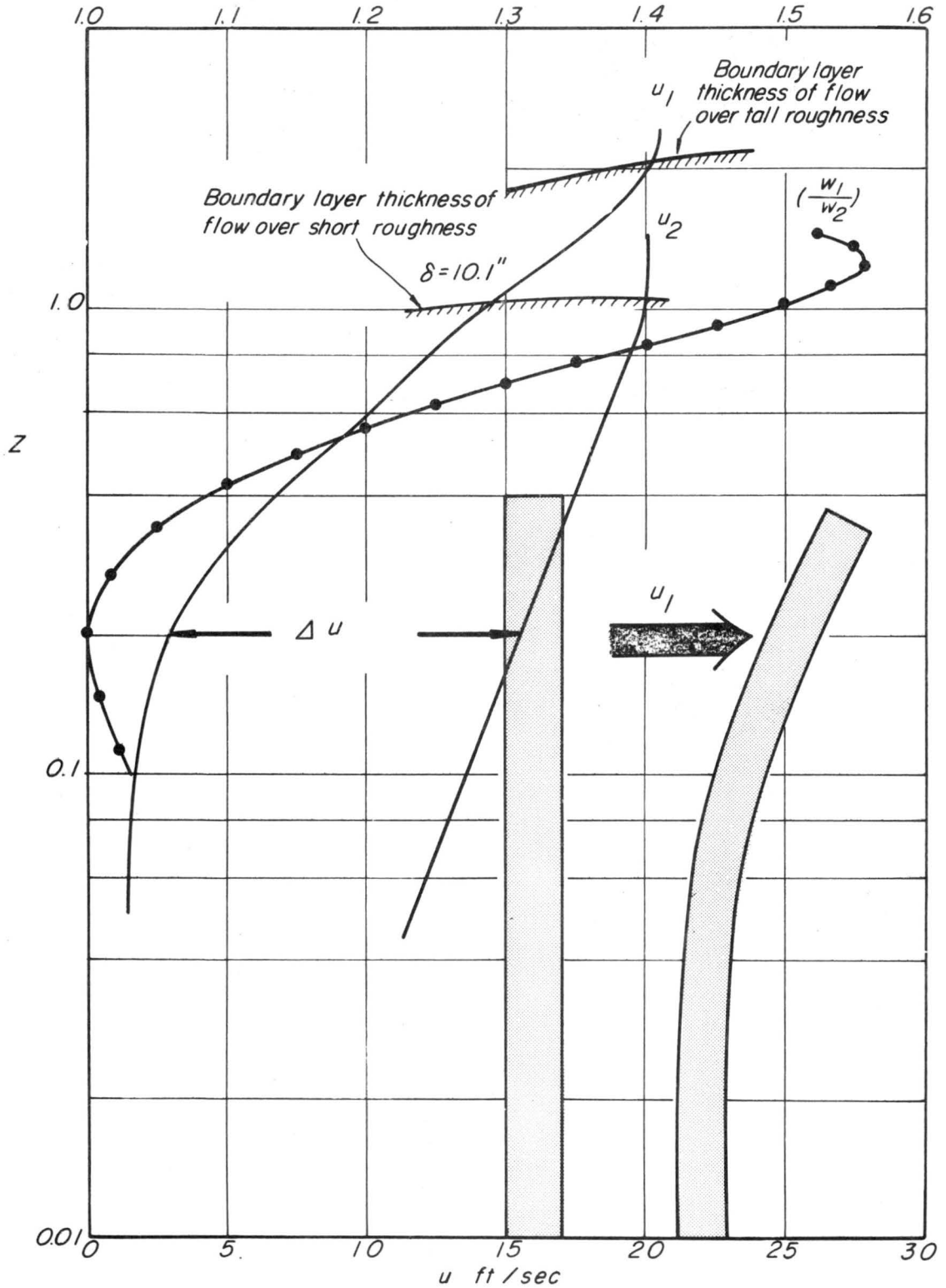

Figure 5-2 Schematic expression of inner and outer fluid flow over a rough surface of tall elements

APPENDIX

APPENDIX

Consider the equation

$$C_s + A \log_{10} C_s = A \log_{10} R_\delta + D \quad . \tag{1}$$

We assume that C_s has the form

$$C_s = A \log_{10} R_\delta - f(R_\delta) + D \quad , \tag{2}$$

where $f(R_\delta)$ is an unknown function.

The substitution of (2) into (1), yields

$$A \log_{10} \left[A \log_{10} R_\delta - f(R_\delta) + D \right] = f(R_\delta) \quad . \tag{3}$$

We then make the substitution

$$f(R_\delta) = A \log_{10} \left[F(R_\delta) \cdot R_\delta \right] \quad , \tag{4}$$

where $F(R_\delta)$ is another unknown function and is regarded as being less than 1.

The substitution of (4) into (3), yields

$$A \log \left[D - A \log F(R_\delta) \right] = A \log \left[F(R_\delta) \cdot R_\delta \right] \quad . \tag{5}$$

On the other hand, C_s can be expressed by means of (2) and (4) as

$$C_s = - A \log_{10} F + D \quad . \tag{6}$$

From (5) we obtain

$$D - A \log_{10} F = F \cdot R_\delta \quad . \tag{7}$$

It is then assumed that F has the form

$$F(R_\delta) = e^{-\alpha(R_\delta)} \tag{8}$$

where the range of α is restricted to $0 < \alpha < 1$.

For sufficiently small values of α , $F(R_\delta)$ may be approximated by

$$F(R_\delta) = 1 - \alpha \tag{9}$$

The substitution of (8) and (9) into (7), yields

$$D + 2.5\alpha = (1 - \alpha) \cdot R_\delta \ . \tag{10}$$

Thus, from (9) and (10), $F(R_\delta)$ can be expressed by

$$F(R_\delta) = \frac{2.5 + D}{R_\delta + 2.5} \ . \tag{11}$$

When (11) is substituted into (6), C_s becomes

$$C_s = A \log_{10} (R_\delta + 2.5) - A \log_{10} (2.5 + D) + D \ . \tag{12}$$

Unclassified

Security Classification

DOCUMENT CONTROL DATA - R&D

(Security classification of title, body of abstract and indexing annotation must be entered when the overall report is classified)

1. ORIGINATING ACTIVITY (Corporate author)	2a. REPORT SECURITY CLASSIFICATION
Fluid Dynamics and Diffusion Laboratory College of Engineering, Colorado State University Fort Collins, Colorado 80521	2b. GROUP

3. REPORT TITLE

INNER AND OUTER FLOW VELOCITY DISTRIBUTIONS THROUGH TALL SIMULATED VEGETATION

4. DESCRIPTIVE NOTES (Type of report and inclusive dates)

Technical Report

5. AUTHOR(S) (Last name, first name, initial)

S. Ito and J. E. Cermak

6. REPORT DATE	7a. TOTAL NO. OF PAGES	7b. NO. OF REFS
April 1968	54	10

8a. CONTRACT OR GRANT NO.	9a. ORIGINATOR'S REPORT NUMBER(S)
DA-AMC-28-043-65-G20 b. PROJECT NO. 2246 c. d.	9b. OTHER REPORT NO(S) (Any other numbers that may be assigned this report)

10. AVAILABILITY/LIMITATION NOTICES

Distribution of This Report is Unlimited

11. SUPPLEMENTARY NOTES	12. SPONSORING MILITARY ACTIVITY
	U. S. Army Materiel Command

13. ABSTRACT

The velocity distribution in and above model vegetation is the subject of this study. Experiments have revealed that flow over a surface which has been made rough by covering it with tall simulated plants may have a universal distribution law. It is suggested that this law can be expressed in terms of the two parameters $\left(\frac{\Delta u}{V_*}\right)_{max}$ and η_o, which in turn depend on the shape, height, and spacing of the cover elements.

DD FORM 1 JAN 64 1473

Unclassified

Security Classification

14. KEY WORDS	LINK A		LINK B		LINK C	
	ROLE	WT	ROLE	WT	ROLE	WT

INSTRUCTIONS

1. ORIGINATING ACTIVITY: Enter the name and address of the contractor, subcontractor, grantee, Department of Defense activity or other organization *(corporate author)* issuing the report.

2*a*. REPORT SECURITY CLASSIFICATION: Enter the overall security classification of the report. Indicate whether "Restricted Data" is included. Marking is to be in accordance with appropriate security regulations.

2*b*. GROUP: Automatic downgrading is specified in DoD Directive 5200.10 and Armed Forces Industrial Manual. Enter the group number. Also, when applicable, show that optional markings have been used for Group 3 and Group 4 as authorized.

3. REPORT TITLE: Enter the complete report title in all capital letters. Titles in all cases should be unclassified. If a meaningful title cannot be selected without classification, show title classification in all capitals in parenthesis immediately following the title.

4. DESCRIPTIVE NOTES: If appropriate, enter the type of report, e.g., interim, progress, summary, annual, or final. Give the inclusive dates when a specific reporting period is covered.

5. AUTHOR(S): Enter the name(s) of author(s) as shown on or in the report. Enter last name, first name, middle initial. If military, show rank and branch of service. The name of the principal author is an absolute minimum requirement.

6. REPORT DATE: Enter the date of the report as day, month, year; or month, year. If more than one date appears on the report, use date of publication.

7*a*. TOTAL NUMBER OF PAGES: The total page count should follow normal pagination procedures, i.e., enter the number of pages containing information.

7*b*. NUMBER OF REFERENCES: Enter the total number of references cited in the report.

8*a*. CONTRACT OR GRANT NUMBER: If appropriate, enter the applicable number of the contract or grant under which the report was written.

8*b*, 8*c*, & 8*d*. PROJECT NUMBER: Enter the appropriate military department identification, such as project number, subproject number, system numbers, task number, etc.

9*a*. ORIGINATOR'S REPORT NUMBER(S): Enter the official report number by which the document will be identified and controlled by the originating activity. This number must be unique to this report.

9*b*. OTHER REPORT NUMBER(S): If the report has been assigned any other report numbers *(either by the originator or by the sponsor)*, also enter this number(s).

10. AVAILABILITY/LIMITATION NOTICES: Enter any limitations on further dissemination of the report, other than those imposed by security classification, using standard statements such as:

(1) "Qualified requesters may obtain copies of this report from DDC."

(2) "Foreign announcement and dissemination of this report by DDC is not authorized."

(3) "U. S. Government agencies may obtain copies of this report directly from DDC. Other qualified DDC users shall request through _____."

(4) "U. S. military agencies may obtain copies of this report directly from DDC. Other qualified users shall request through _____."

(5) "All distribution of this report is controlled. Qualified DDC users shall request through _____."

If the report has been furnished to the Office of Technical Services Department of Commerce, for sale to the public, indicate this fact and enter the price, if known.

11. SUPPLEMENTARY NOTES: Use for additional explanatory notes.

12. SPONSORING MILITARY ACTIVITY: Enter the name of the departmental project office or laboratory sponsoring *(paying for)* the research and development. Include address.

13. ABSTRACT: Enter an abstract giving a brief and factual summary of the document indicative of the report, even though it may also appear elsewhere in the body of the technical report. If additional space is required, a continuation sheet shall be attached.

It is highly desirable that the abstract of classified reports be unclassified. Each paragraph of the abstract shall end with an indication of the military security classification of the information in the paragraph, represented as *(TS)*, *(S)*, *(C)*, *or (U)*.

There is no limitation on the length of the abstract. However, the suggested length is from 150 to 225 words.

14. KEY WORDS: Key words are technically meaningful terms or short phrases that characterize a report and may be used as index entries for cataloging the report. Key words must be selected so that no security classification is required. Idenfiers, such as equipment model designation, trade name, military project code name, geographic location, may be used as key words but will be followed by an indication of technical context. The assignment of links, rules, and weights is optional.

MINIMUM BASIC DISTRIBUTION LIST FOR USAMC SCIENTIFIC AND TECHNICAL REPORTS IN METEOROLOGY AND ATMOSPHERIC SCIENCES

Commanding General (1)
U. S. Army Materiel Command
Attn: AMCRD-RV-A
Washington, D. C. 20315

Commanding General (1)
U. S. Army Electronics Command
Attn: AMSEL-EW
Fort Monmouth, New Jersey 07703

Commanding General (1)
U. S. Army Test and Evaluation Command
Attn: NBC Directorate
Aberdeen Proving Ground, Maryland 21005

Commanding Officer (1)
U. S. Army Ballistics Research Laboratories
Attn: AMXBR-IA
Aberdeen Proving Ground, Maryland 21005

Chief, Atmospheric Physics Division (2)
Atmospheric Sciences Laboratory
U. S. Army Electronics Command
Fort Monmouth, New Jersey 07703

U. S. Army Munitions Command (1)
Attn: Irving Solomon
Operations Research Group
Edgewood Arsenal, Maryland 21010

Commanding Officer (1)
U. S. Army Dugway Proving Ground
Attn: Meteorology Division
Dugway, Utah 84022

Commanding Officer (1)
U. S. Army CDC, CBR Agency
Attn: Mr. N. W. Bush
Fort McClellan, Alabama 36205

Commanding General (1)
U. S. Army Test and Evaluation Command
Attn: AMSTE-EL
Aberdeen Proving Ground, Maryland 21005

Commandant (1)
U. S. Army Signal School
Attn: Meteorological Department
Fort Monmouth, New Jersey 07703

Assistant Chief of Staff for Force Development (1)
CBR Nuclear Operations Directorate
Department of the Army
Washington, D. C. 20310

Director (1)
Atmospheric Sciences Programs
National Sciences Foundation
Washington, D. C. 20550

Assistant Secretary of Defense (1)
Research and Engineering
Attn: Technical Library
Washington, D. C. 20301

R. A. Taft Sanitary Engineering Center (1)
Public Health Service
4676 Columbia Parkway
Cincinnati, Ohio

Dr. Hans A. Panofsky (1)
Department of Meteorology
The Pennsylvania State University
University Park, Pennsylvania

Commanding General (1)
U. S. Continental Army Command
Attn: Reconnaissance Branch ODCS for Intelligence
Fort Monroe, Virginia 23351

Commander (1)
Air Force Cambridge Research Laboratories
Attn: CRZW
1065 Main Street
Waltham, Massachusetts

President (1)
U. S. Army Artillery Board
Fort Sill, Oklahoma 73504

National Center for Atmospheric Research (1)
Attn: Library
Boulder, Colorado

Dr. J. E. Cermak, Head (15)
Fluid Mechanics Program
Colorado State University
Fort Collins, Colorado 80521

Author (1)

Chief of Research and Development (1)
Department of the Army
Attn: CRD/M
Washington, D. C. 20310

Commanding General (1)
U. S. Army Missile Command
Attn: AMSMI-RRA
Redstone Arsenal, Alabama 35809

Commanding General (1)
U. S. Army Natick Laboratories
Attn: Earth Sciences Division
Natick, Massachusetts 01762

Director, U. S. Army Engineer (1)
Waterways Experiment Station
Attn: WES-FV
Vicksburg, Mississippi 39181

Chief, Atmospheric Sciences Research Division (5)
Atmospheric Sciences Laboratory
U. S. Army Electronics Command
Fort Huachuca, Arizona 85613

Commanding Officer (1)
U. S. Army Frankford Arsenal
Attn: SMUFA-1140
Philadelphia, Pennsylvania 19137

Commandant (1)
U. S. Army Artillery and Missile School
Attn: Target Acquisition Department
Fort Sill, Oklahoma 73504

Commanding General (1)
U. S. Army Electronics Proving Ground
Attn: Field Test Department
Fort Huachuca, Arizona 85613

Commanding General (1)
U. S. Army Test and Evaluation Command
Attn: AMSTE-BAF
Aberdeen Proving Ground, Maryland 21005

Office of Chief Communications - Electronics (1)
Department of the Army
Attn: Electronics Systems Directorate
Washington, D. C. 20315

Chief of Naval Operations (1)
Department of the Navy
Attn: Code 427
Washington, D. C. 20350

Director (1)
Bureau of Research and Development
Federal Aviation Agency
Washington, D. C. 20553

Director of Meteorological Systems (1)
Office of Applications (FM)
National Aeronautics and Space Administration
Washington, D. C. 20546

Director (1)
Atmospheric Physics and Chemistry Laboratory
Environmental Science Services Administration
Boulder, Colorado

Andrew Morse (1)
Army Aeronautical Activity
Ames Research Center
Moffett Field, California 94035

Commanding Officer (2)
U. S. Army Cold Regions Research and Engineering Laboratories
Attn: Environmental Research Branch
Hanover, New Hampshire 03755

Mr. Ned L. Kragness (1)
U. S. Army Aviation Materiel Command
SMOSM-E
12th and Spruce Streets
Saint Louis, Missouri 63166

Commanding Officer, U. S. Army (1)
Artillery Combat Development Agency
Fort Sill, Oklahoma 73504

Commander, USAR Air Weather Service (MATS) (1)
Attn: AWSSS/TIPD
Scott Air Force Base, Illinois

Dr. John Bogusky (1)
7310 Cedardale Drive
Alexandria, Virginia 22308

Commanding General (1)
U. S. Army Combat Development Command
Attn: CDCMR-E
Fort Belvoir, Virginia 22060

Commanding General (1)
U. S. Army Munitions Command
Attn: AMSMU-RE-R
Dover, New Jersey 07801

Commanding Officer (1)
U. S. Army Ballistics Research Laboratories
Attn: AMXBR-B
Aberdeen Proving Ground, Maryland 21005

Director (2)
Atmospheric Sciences Laboratory
U. S. Army Electronics Command
Fort Monmouth, New Jersey 07703

Chief, Atmospheric Sciences Office (2)
Atmospheric Sciences Laboratory
U. S. Army Electronics Command
White Sands Missile Range, New Mexico 88002

Commanding Officer (1)
U. S. Army Picatinny Arsenal
Attn: SMUPA-TV-3
Dover, New Jersey 07801

Commanding Officer (1)
U. S. Army Communications - Electronics Combat Development Agency
Fort Monmouth, New Jersey 07703

Commanding General (1)
Deseret Test Center
Attn: Design and Analysis Division
Fort Douglas, Utah 84113

Commandant (1)
U. S. Army CBR School Micrometeorological Section
Fort McClellan, Alabama 36205

Assistant Chief of Staff for Intelligence (1)
Department of the Army
Attn: ACSI-DERSI
Washington, D. C. 20310

Officer in Charge (1)
U. S. Naval Weather Research Facility
U. S. Naval Air Station, Building 4-28
Norfolk, Virginia 23500

Chief, Fallout Studies Branch (1)
Division of Biology and Medicine
Atomic Energy Commission
Washington, D. C. 20545

Director (1)
U. S. Weather Bureau
Attn: Librarian
Washington, D. C. 20235

Dr. Albert Miller (1)
Department of Meteorology
San Jose State College
San Jose, California 95114

Mrs. Francis L. Wheedon (1)
Army Research Office
3045 Columbia Pike
Arlington, Virginia 22201

Commander (1)
Air Force Cambridge Research Laboratories
Attn: CRXL
L. G. Hanscom Field
Bedford, Massachusetts

Harry Moses, Asso. Meteorologist (1)
Radiological Physics Division
Argonne National Laboratory
9700 S. Cass Avenue
Argonne, Illinois 60440

Defense Documentation Center (20)
Cameron Station
Alexandria, Virginia 22314

Office of U. S. Naval Weather Service (1)
U. S. Naval Air Station
Washington, D. C. 20390

Dr. Gerald Gill (1)
University of Michigan
Ann Arbor, Michigan 48103